CHAPTER-4

Mononuclear five-coordinate Cobalt(II) Complexes with N_4-coordinate pyrazole based ligand and pseudohalides: Syntheses, Structures, DNA and Protein Binding study.

Abstract

A series of mononuclear five coordinated cobalt(II) complexes of the type [Co(dbdmp)(X)]Y, where dbdmp = *N*,*N*-diethyl-*N'*,*N'*-bis((3,5-dimethyl-*1H*-pyrazol-1-yl)methyl)ethane-1,2-diamine, X = N_3^- / NCO^- / NCS^- and Y = PF_6^- / BF_4^- / ClO_4^- have been synthesized and characterized by microanalyses and spectroscopic techniques. Crystal structures of the complexes $[Co(N_3)(dbdmp)]PF_6$ (**1**), $[Co(N_3)(dbdmp)]ClO_4$ (**3**), $[Co(NCO)(dbdmp)]PF_6$ (**4**), $[Co(NCO)(dbdmp)]ClO_4$ (**6**) and $[Co(NCS)(dbdmp)]ClO_4$ (**9**) have been solved by single crystal X-ray diffraction studies and showed that all the complexes have distorted trigonal bipyramidal geometry and PF_6^- counter anion containing complexes $[Co(N_3)(dbdmp)]PF_6$ (**1**) and $[Co(NCO)(dbdmp)]PF_6$ (**4**) have chiral space group. The binding ability of synthesized complexes with CT-DNA and BSA has been studied by spectroscopic methods and viscosity measurements. The experimental results of absorption titration of cobalt(II) complexes with CT-DNA indicate that the complexes have ability to form adducts and they can stabilize the DNA helix. The cobalt(II) complexes exhibit good binding propensity to bovine serum albumin (BSA) protein.

4.1. Introduction

During the last few decades, synthesis of new transition metal complexes as anticancer agent constitutes an important area of research. Transition metal complexes have been used to study the interaction with DNA because of their versatile coordination mode, redox and structural properties. DNA is also a good target for metal complexes because of its wide variety of binding sites [1-4]. Cobalt is an essential element in the biological system and it regulates the synthesis of DNA indirectly as it is an active center of vitamin B12. The interaction of DNA with cobalt complexes with nitrogen based ligand has attracted much attention recently [5-6]. There are many reports on the interaction of DNA with copper(II) complexes but there are few reports on DNA binding with cobalt(II) [7-12] and cobalt(III) complexes [13-17] based on nitrogen and oxygen containing ligand.

Nitrogen containing heterocyclic compound like imidazole or pyrazole plays an important role in biological system. Although pseudohalides are ambidentate ligand, we always obtain mononuclear cobalt(II) complexes, like copper(II) complexes, in presence of pyrazole containing tripodal ligand and pseudohalides such as azide or thiocyanate or isocyanate ion. The objective of the work was to investigate whether cobalt(II) complexes with same ligand and pseudohalides have any interaction with DNA and BSA.

In the present chapter, we report on the syntheses, characterizations and X-ray crystal structures of mononuclear cobalt(II) complexes of the type [Co(dbdmp)X]Y, where dbdmp = *N*,*N*-diethyl-*N'*,*N'*-bis((3,5-dimethyl-*1H*-pyrazol-1-yl)methyl)ethane-1,2-diamine, a tetradentate N_4-coordinated ligand, X = N_3^- / NCO^- / NCS^- and Y = PF_6^- / BF_4^- / ClO_4^-. Crystal structure of the complexes $[Co(N_3)(dbdmp)]PF_6$(**1**), $[Co(N_3)(dbdmp)]ClO_4$ (**3**), $[Co(NCO)(dbdmp)]PF_6$ (**4**), $[Co(NCO)(dbdmp)]ClO_4$ (**6**) and $[Co(NCS)(dbdmp)]ClO_4$ (**9**) have been solved by single crystal X-ray diffraction studies and showed that all the complexes have distorted trigonal bipyramidal geometry. The DNA binding study of the complexes were explored by absorption and fluorescence spectroscopy and protein (BSA) binding study by fluorescence spectroscopy. The interaction of CT-DNA with cobalt(II) complexes by absorption spectroscopy shows several isobestic points indicating the formation of new complexes with DNA and cobalt(II).

4.2. Experimental

4.2.1. Materials

The chemicals and solvents were of analytical grade and purchased from commercial sources. $Co(CH_3COO)_2.4H_2O$ (Qualigens, India), Bovin serum albumin (BSA) (Spectrochem, India) were of reagent grade and used as received. $Co(ClO_4)_2.6H_2O$ was prepared by reaction of cobalt carbonate with dilute $HClO_4$ acid and followed by slow evaporation of the solution.

Caution! Transition metal complex with azide ion and organic ligands are potentially explosive. Only a small amount of material should be synthesized and it should be handled with care.

4.2.2. Syntheses of Complexes

4.2.2.1. $[Co(N_3)(dbdmp)]X$, X = PF_6^- (1) and BF_4^- (2).

A methanol solution (10 ml) of ligand dbdmp (0.166 g, 0.5 mmol) was added dropwise to a stirring solution of $Co(CH_3COO)_2.4H_2O$ (0.125 g, 0.5 mmol) in the same solvent (10 ml). To this solution, NaN_3 (0.032 g, 0.5 mmol) in water (0.5 ml) was added slowly. After 10 min, NH_4PF_6 / NH_4BF_4 (0.5 mmol) in water (1 ml) was added and the blue coloured solution was stirred for 4 h, filtered and kept at room temperature for slow evaporation. Plate shape dark brown coloured X-ray quality single crystals were obtained after seven days.

$[Co(N_3)(dbdmp)]PF_6$ (1) : Yield. 0.120 g (41 %). Found: C = 37.25, H = 5.59, N = 21.96 %. Anal calc for $C_{18}H_{32}N_9PF_6Co$: C = 37.38, H = 5.58, N = 21.79 %. IR (KBr pellet) cm^{-1}; $\nu(N_3^-)$, 2072 vs; ν(C = C) + ν (C = N)/pz ring, 1554 s, 1467 s; $\nu(PF_6^-)$, 845 br. UV-Vis spectra: $\lambda_{max}(CH_3CN)$/nm (ε_{max}/$mol^{-1}cm^{-1}$). 781 (30), 606 (232), 502 (109), 332 (1099), 249 (3698). Λ_M (CH_3CN)($\Omega^{-1}cm^2$ mol^{-1}) = 122. μ_{eff} = 4.27 BM.

$[Co(N_3)(dbdmp)]BF_4$ (2) : Yield. 0.155 g (60 %). Found: C = 41.75, H = 6.19, N = 24.46 %. Anal calc for $C_{18}H_{32}N_9BF_4Co$: C = 41.56, H = 6.20, N = 24.23 %. IR (KBr pellet) cm^{-1}; $\nu(N_3^-)$, 2065 vs; ν(C = C) + ν (C = N)/pz ring, 1551 s, 1466 s; $\nu(BF_4^-)$, 1028-1068 br. UV-Vis spectra: $\lambda_{max}(CH_3CN)$/nm (ε_{max}/$mol^{-1}cm^{-1}$). 780 (39),

606 (305), 502 (147), 332 (1409), 243 (3652). Λ_M (CH_3CN)($\Omega^{-1}cm^2$ mol^{-1}) = 120. μ_{eff} = 4.16 BM.

4.2.2.2. [Co(N_3)(dbdmp)]ClO_4 (3)

A methanol solution (10 ml) of ligand dbdmp (0.166 g, 0.5 mmol) was added drop wise to a stirring $Co(ClO_4)_2.6H_2O$ (0.182 g, 0.5 mmol) solution (10 ml) in the same solvent. To this solution, NaN_3 (0.032 g, 0.5 mmol) in water (1 ml) was added slowly and blue colored solution was stirred for 4 h, filtered and kept at room temperature for slow evaporation. Blue colored single crystals were collected after 5 days. Yield. 0.140 g (41 %). Found C = 40.55, H = 5.99, N = 23.43 %, Anal calc for $C_{18}H_{32}N_9ClO_4Co$: C = 40.57, H = 6.05, N = 23.66 %. IR (KBr pellet) cm^{-1}; ν(N_3^-), 2067 vs; ν(C = C) + ν(C = N)/pz ring, 1558 s, 1549 s, 1463 s; ν_{asmy}(Cl–O), 1078 br; δ(O–Cl–O), 624 s. UV-Vis spectra: λ_{max}(CH_3CN)/nm (ε_{max}/$mol^{-1}cm^{-1}$). 778 (33), 606 (276), 502 (128), 332 (1288), 242 (3741). Λ_M(CH_3CN)($\Omega^{-1}cm^2$ mol^{-1}) = 118. μ_{eff} = 4.24 BM.

4.2.2.3. [Co(NCO)(dbdmp)]PF_6 (4)

To a stirring solution of $Co(CH_3COO)_2.4H_2O$ (0.125 g, 0.5 mmol) in methanol (10 ml), ligand dbdmp (0.166 g, 0.5 mmol) in methanol was added drop by drop. After 10 min, NaNCO (0.032 g, 0.5 mmol) in water (0.5 ml) was added. Finally, NH_4PF_6 (0.082 g, 0.5 mmol) in water (0.5 ml) was added to the solution. This blue coloured solution was stirred for 4 h, filtered and kept for slow evaporation. Plate shape dark blue coloured X-ray quality single crystals were obtained after seven days. Yield. 0.139 g (48 %). Found: C = 39.57, H = 5.59, N = 16.90 %. Anal calc for $C_{19}H_{32}N_7OPF_6Co$: C = 39.45, H = 5.58, N = 16.95 %. IR (KBr pellet) cm^{-1}; ν(NCO^-), 2229 vs; ν(C = C) + ν (C = N)/py ring, 1553 s, 1466 s; ν(PF_6^-), 845 br. UV-Vis spectra: λ_{max}(CH_3CN)/nm (ε_{max}/$mol^{-1}cm^{-1}$). 765 (34), 599 (195), 489 (138), 243 (3461). Λ_M ($\Omega^{-1}cm^2$ mol^{-1}) = 116. μ_{eff} = 4.19 BM.

4.2.2.4. [Co(NCO)(dbdmp)]BF_4 (5)

This complex was prepared by following the same procedure as for complex **2** except NH_4BF_4 was used in the place of NH_4PF_6. Dark blue coloured crystals were obtained. Yield. 0.167 g (64 %). Found: C = 43.97, H = 6.13, N = 18.96 %. Anal calc for $C_{19}H_{32}N_7OBF_4Co$: C = 43.86, H = 6.20, N = 18.85 %. IR (KBr pellet) cm^{-1}; ν(NCO^-), 2214 vs; ν(C = C) + ν (C = N)/pz ring, 1553 s, 1466 s; ν(BF_4^-), 1068 br.

UV-Vis spectra: λ_{max}(CH_3CN)/nm (ε_{max}/$mol^{-1}cm^{-1}$). 766 (41), 599 (230), 489 (158), 245 (3448). Λ_M (CH_3CN)($\Omega^{-1}cm^2\ mol^{-1}$) = 116. μ_{eff} = 4.31 BM.

4.2.2.5. [Co(NCO)(dbdmp)]ClO_4 (6)

This complex was prepared by following the same procedure as for complex **3** except NaNCO was used in the place of NaN_3. Dark blue coloured crystals were obtained after one week. Yield 0.150 g (58 %). Found: C = 42.87, H = 6.11, N = 18.61 %, Anal calc for $C_{19}H_{32}N_7O_5ClCo$: C = 42.82, H = 6.05, N = 18.40 %. IR (KBr pellet) cm^{-1}; ν(NCO^-), 2218 vs; ν(C = C) + ν (C = N)/py ring, 1553 s, 1466 s; ν_{asmy}(Cl–O), 1076 br; δ(O–Cl–O), 624 s. UV-Vis spectra: λ_{max}(CH_3CN)/nm (ε_{max}/$mol^{-1}cm^{-1}$). 772 (39), 599 (237), 489 (154), 245(3517), 228 (3473). Λ_M ($\Omega^{-1}cm^2\ mol^{-1}$) = 122. μ_{eff} = 4.18 BM.

4.2.2.6. [Co(NCS)(dbdmp)]X, X = PF_6^- (7) and BF_4^- (8)

This complex was prepared by following the same procedure as for complex **1** except KSCN was used in the place of NaN_3.

[Co(NCS)(dbdmp)]PF_6 (7) : Yield. 0.175 g (59 %). Found: C = 38.27, H = 5.50, N = 16.36 %. Anal calc for $C_{19}H_{32}N_7SPF_6Co$: C = 38.39, H = 5.43, N = 16.49 %. IR (KBr pellet) cm^{-1}; ν(NCS^-), 2067 vs; ν(C = C) + ν (C = N)/pz ring, 1554 s, 1467 s; ν(PF_6^-), 846 br. UV-Vis spectra: λ_{max} (CH_3CN)/nm (ε_{max}/$mol^{-1}cm^{-1}$). 723 (45), 580 (382), 489 (153), 319 (2408), 246 (3762), 218 (3567). Λ_M (CH_3CN)($\Omega^{-1}cm^2\ mol^{-1}$) = 119. μ_{eff} = 4.22 BM.

[Co(NCS)(dbdmp)]BF_4 (8) : Yield. 0.148 g (55 %). Found: C = 42.77, H = 5.99, N =18.06 %. Anal calc for $C_{19}H_{32}N_7SBF_4Co$: C = 42.55, H = 6.01, N = 18.28 %. IR (KBr pellet) cm^{-1}; ν(NCS^-), 2065 vs; ν(C = C) + ν (C = N)/pz ring, 1558 s, 1552 s, 1467 s; ν(BF_4^-), 1083 br. UV-Vis spectra: λ_{max}(CH_3CN)/nm (ε_{max}/$mol^{-1}cm^{-1}$). 724 (49), 580 (407), 489 (165), 319 (2540), 249 (3845), 219 (3627). Λ_M (CH_3CN) ($\Omega^{-1}cm^2mol^{-1}$) = 122. μ_{eff} = 4.26 BM.

4.2.2.7. [Co(NCS)(dbdmp)]ClO_4 (9)

This complex was prepared by following the same procedure as for complex **3** except KSCN was used instead of NaN_3. Yield. 0.165 g (64 %). Found C = 41.82, H = 5.90, N = 17.75 %. Anal calc for $C_{19}H_{32}N_7O_4ClSCo$: C = 41.57, H = 5.88, N = 17.86 %. IR (KBr pellet) cm^{-1}; ν(NCS^-), 2066 vs; ν(C = C) + ν (C = N)/pz ring, 1553 s, 1466 s; ν_{asmy}(Cl–O), 1068; δ(O–Cl–O), 624 s. UV-Vis spectra: λ_{max} (CH_3CN)/nm (ε_{max}/$mol^{-1}cm^{-1}$). 726 (45), 580 (393), 492 (156), 318 (2453), 251 (3652), 218 (3460). Λ_M (CH_3CN) ($\Omega^{-1}cm^2\,mol^{-1}$) = 118. μ_{eff} = 4.32 BM.

4.2.3. Physical Measurements

The IR spectra were recorded on a Perkin-Elmer FT-IR spectrometer RX1 spectrum using KBr pellets. The micro analyses (C, H and N) were carried out using a Perkin-Elmer IA 2400 series elemental analyzer. UV-Vis spectra (900 - 190 nm) were recorded on a Perkin-Elmer spectrophotometer model Lambda 35 in acetonitrile solution. Solution conductivity were measured in acetonitrile solution (10^{-3} M) using Equip-Tronics conductivity meter (model no. EQ-660A). Room temperature magnetic susceptibilities of powder samples were measured using Guoy balance using $Hg[Co(SCN)_4]$ as the reference.

4.2.4. DNA and BSA Binding Experiments

All the spectral titration experiments involving interaction of the complexes with CT-DNA were performed in double distilled buffer containing 50 mM Tris – HCl, 150 mM NaCl and adjusted to pH 7.2 with 1M hydrochloric acid. Stock solutions of cobalt(II) complexes were prepared in DMF. A solution of CT-DNA in buffer gave a ratio of UV absorption at 260 and 280 nm of ca. 1.9 : 1, indicating that DNA was sufficiently free from protein. The DNA concentration per nucleotide was determined by absorption spectroscopy with the molar absorption coefficient 6600 M^{-1} cm^{-1} at 260 nm [18-19].

4.2.4.1. Absorption Spectroscopic Studies

The detail of this section is given in Chapter-3 (Section 2.4.1).

4.2.4.2. Fluorescence Spectroscopic Studies

The detail of this section is given in Chapter-3 (Section 2.4.2).

4.2.4.3. Viscosity Measurements

Viscosity experiments were carried out using Ostwald's capillary viscometer, immersed in a thermostated water bath with the temperature setting at 30±0.01°C and flow time was measured using digital stopwatch. The flow time of DNA solution was corrected by subtracting the flow time observed for the buffer solution. The viscosity of DNA solution has been measured in the presence of increasing amount of cobalt(II) complexes. Each sample was measured three times and an average flow time was calculated. Data were represented as (η/η_0) versus binding ratio of cobalt(II) complex to DNA, where η is a viscosity of DNA in the presence of complex and η_0 is the viscosity of DNA alone.

4.2.4.4. Protein (Bovine Serum Albumin) Binding Experiments

The protein binding studies have been performed by tryptophan fluorescence quenching experiments using bovine (BSA, 50 μM, based on its molecular mass of 66,000 Da) in buffer (containing 50 mM Tris-buffer and 150 mM NaCl in pure aqueous medium at pH 7.2). BSA was kept in the dark at 277 K. Double distilled water was used throughout the experiment. The quenching of the emission intensity of tryptophan residue of BSA at 343 nm was monitored using complexes **1, 4** and **7** in DMF as quenchers with increasing concentrations [20]. Fluorescence spectra were recorded from 290 nm to 450 nm with an excitation wavelength of 290 nm on a model HITACHI, F-7000 fluorescence spectrophotometer.

4.3. X-ray Crystallography

The crystallographic data, details of data collection and some important features of the refinement for the compound **1**, **3, 4, 6** and **9** are given in Table 4.1 and selected bond lengths and angles are given in Table 4.2. Crystals of suitable size of complexes **1**, **3, 4, 6** and **9** were obtained by slow evaporation of methanol solution. For complexes **1**, **4** and **6**, data were collected on a Bruker SMART APEX diffractometer equipped with CCD area detector at 110 K and 296 K respectively and

Oxford X-CALIBUR-S diffractometer for complexes **3** and **9** with Mo-K_α radiation (λ = 0.71073Å) and Cu-K_α radiation (λ = 1.541841Å) at 293 K, respectively. The data interpretation was processed with SAINT software [21] and CrysAlisPro, Agilent Technologies, Version 1.171.35.19 [22]. Empirical absorption correction was applied with SADABS software programs [23]. All structures were solved by direct methods using SHELXTL [24] and refined by the full-matrix least-square based on F^2 technique using SHELXL-97 program package [25]. All non-hydrogen atoms were refined anisotropically. The positions of the hydrogen atoms either were calculated from the difference Fourier map or were introduced at calculated positions as riding on bonded atoms.

4.4. Results and Discussions

4.4.1. Syntheses

The mononuclear pentacoordinated pseudohalide containing cobalt(II) complexes [Co(dbdmp)(X)]Y, (X = N_3^-, NCO^-, NCS^- and Y = PF_6^-, BF_4^-, ClO_4^-) were readily synthesized through reaction of cobalt(II) salt such as $Co(ClO_4)_2.6H_2O$ or $Co(CH_3COO)_2.4H_2O$, tetradentate N_4- coordinated ligand dbdmp, pseudohalides X (N_3^- / NCO^- / NCS^-) and counter anion Y (PF_6^- / BF_4^- / ClO_4^-) ions in 1 : 1 : 1 : 1 mole ratio in presence of aqueous methanol at room temperature [Scheme 4.1]. There are only few reports on five-coordinated cobalt(II) complexes with nitrogen coordinating ligand [26-35]. We have synthesized and structurally characterized few new five-coordinated cobalt(II) complexes with trigonal bipyramidal geometry using tetradentate N_4-coordinate ligand and pseudohalides. The important point is that when the complexes [Co(dbdmp)(X)]PF_6 (X = N_3^- and NCO^-) are synthesized by reacting $Co(CH_3COO)_2.4H_2O$, ligand dbdmp, X^- and PF_6^- ions, the complexes [Co(N_3)(dbdmp)]PF_6 (**1**) and [Co(NCO)(dbdmp)]PF_6 (**4**) have chiral space group. But when the complexes [Co(dbdmp)(X)]ClO_4 (X = N_3^-, NCO^-, NCS^-) are synthesized by using $Co(ClO_4)_2.6H_2O$, ligand dbdmp and X^-, the complexes have non-chiral space group.

Table 4.1. Crystal parameters of complexes **1**, **3**, **4, 6** and **9.**

Empirical formula	$C_{36}H_{64}N_{18}F_{12}P_2Co_2$ **(1)**	$C_{18}H_{32}CoN_9ClO_4$ **(3)**	$C_{19}H_{32}CoN_7F_6OP$ **(4)**	$C_{19}H_{32}CoN_7ClO_5$ **(6)**	$C_{19}H_{32}CoN_7ClO_4S$ **(9)**
Formula weight	1156.85	532.91	578.42	532.90	548.96
Temperature (K)	110(2)	293	110(2)	296(2)	293(2)
Wavelength (Å)	0.71073	0.71073	0.71073	0.71073	1.54184
Crystal system	Monoclinic	Monoclinic	Orthorhombic	Monoclinic	Monoclinic
Space group	*C2*	$P2_1/c$	$P2_12_12_1$	$P2_1/c$	$P2_1/c$
a (Å)	24.851(3)	8.6033(2)	8.2541(12)	8.874(5)	15.0296(4)
b (Å)	10.9025(10)	19.3515(4)	11.1622(16)	19.166(5)	12.0800(4)
c (Å)	20.5434(18)	14.5931(3)	27.594(4)	14.492(5)	14.4785(4)
~, (°)	90	90	90	90	90
(°)	109.596(2)	91.799(2)	90.00	93.613(5)	97.771(3)
¥ (°)	90	90	90	90	90
Volume ($Å^3$)	5243.7(9)	2428.36(9)	2542.3(6)	2459.9(17)	2604.54(13)
Z	4	4	4	4	4
Density (g cm^{-3})	1.465	1.458	1.511	1.439	1.400
Absorption coefficient (mm^{-1})	0.783	0.860	0.808	0.850	7.182

F(000)	2392	910	1196	1116	1148
θ range for data collection (°)	1.05 to 28.27	3.45 to 27.35	1.48 to 27.99	1.76 to 26.41	5.387 to 71.644
Index ranges	$-32 \le h \le 31$, $-14 \le k \le 13$, $-27 \le l \le 26$	$-7 \le h \le 11$ $-23 \le k \le 24$ $-18 \le l \le 18$	$-10 \le h \le 10$, $-14 \le k \le 14$, $-18 \le l \le 35$	$-11 \le h \le 11$, $-23 \le k \le 23$, $-18 \le l \le 18$	$-18 \le h \le 17$, $-11 \le k \le 14$, $-17 \le l \le 11$
Reflections collected	22524	5148	15094	32354	52247
Independent reflections	11578 [*R*(int) = 0.0295]	10204 [*R*(int) = 0.0300]	5808 [*R*(int) = 0.0453]	5029 [*R*(int) = 0.0227	10463 [*R*(int) = 0.0363]
Max. and min. transmission	0.8719 and 0.7712	1.0000 and 0.64654	0.9382 and 0.7820	0.903 and 0.832	0.366and 0.265
Data / restraints / parameters	11578 / 1 / 643	5148 / 0 / 299	5808 / 0 / 322	5029 / 0 / 298	5083/ 0 / 298
Goodness-of-fit on F^2	1.139	1.053	1.181	1.069	1.028
Final R indices [*I*>2sigma(*I*)]	*R1* = 0.0505, *wR1* = 0.1155	*R1* = 0.0421, *wR1* = 0.1144	*R1* = 0.0632, *wR1* = 0.1304	*R1* = 0.0364, *wR1* = 0.1073	*R1* = 0.0608, *wR1* = 0.1518
R indices (all data)	*R2* = 0.0546, *wR2* = 0.1199	*R2* = 0.0509, *wR2* = 0.1226	*R2* = 0.0699, *wR2* = 0.1279	*R2* = 0.0466, *wR2* = 0.1242	*R2* = 0.0820, *wR2* = 0.1699
Largest diff. peak and hole (eA^{-3})	0.967 and -0.423	0.520 and -0.296	0.799 and -0.782	0.416 and -0.332	0.503 and -0.498
Flack parameters	0.034(11)	-----	0.05(2)	-----	-----
CCDC number	890815	949199	890816	991574	996282

Table 4.2. Bond lengths (Å) and bond angles (˚) of Complexes **1**, **3**, **4, 6** and **9.**

Bond Length (Å)					
[Co(N$_3$)(dbdmp)]PF$_6$ (1)				**[Co(N$_3$)(dbdmp)]ClO$_4$ (3)**	
Co(1)-N(7)	2.001(3)	Co(2)-N(16)	1.983(3)	Co(1)-N(7)	1.999(2)
Co(1)-N(1)	2.036(3)	Co(2)-N(14)	2.031(3)	Co(1)-N(1)	2.067(2)
Co(1)-N(5)	2.055(3)	Co(2)-N(10)	2.039(3)	Co(1)-N(5)	2.040(2)
Co(1)-N(6)	2.117(3)	Co(2)-N(15)	2.118(3)	Co(1)-N(6)	2.124(2)
Co(1)-N(3)	2.256(3)	Co(2)-N(12)	2.279(3)	Co(1)-N(3)	2.2435(19)
[Co(NCO)(dbdmp)]PF$_6$ (4)		**[Co(NCO)(dbdmp)]ClO$_4$ (6)**		**[Co(NCS)(dbdmp)]ClO$_4$ (9)**	
Co(1)-N(7)	1.950(4)	Co(1)-N(7)	1.975(3)	Co(1)-N(7)	1.998(3)
Co(1)-N(1)	2.040(3)	Co(1)-N(1)	2.053(2)	Co(1)-N(1)	2.030(3)
Co(1)-N(5)	2.050(3)	Co(1)-N(5)	2.078(2)	Co(1)-N(5)	2.030(3)
Co(1)-N(6)	2.108(3)	Co(1)-N(6)	2.130(2)	Co(1)-N(6)	2.144(3)
Co(1)-N(3)	2.330(3)	Co(1)-N(3)	2.243(2)	Co(1)-N(3)	2.262(3)
C(19)-N(7)	1.147(6)	C(19)-N(7)	1.126(4)	N(7)-C(19)	1.149(5)
C(19)-O(1)	1.205(6)	C(19)-O(5)	1.206(3)	C(19)-S(1)	1.607(4)

Bond Angles (°)

$[Co(N_3)(dbdmp)]PF_6$ (1)				**$[Co(N_3)(dbdmp)]ClO_4$ (3)**	
N(7)-Co(1)-N(1)	104.99(12)	N(16)-Co(2)-N(14)	104.79(13)	N(7)-Co(1)-N(1)	104.31(10)
N(7)-Co(1)-N(5)	102.06(13)	N(16)-Co(2)-N(10)	100.67(13)	N(7)-Co(1)-N(5)	106.80(9)
N(1)-Co(1)-N(5)	118.90(12)	N(14)-Co(2)-N(10)	115.65(12)	N(1)-Co(1)-N(5)	112.17(8)
N(7)-Co(1)-N(6)	96.14(13)	N(16)-Co(2)-N(15)	99.63(14)	N(7)-Co(1)-N(6)	95.75(9)
N(1)-Co(1)-N(6)	119.29(12)	N(14)-Co(2)-N(15)	120.93(12)	N(1)-Co(1)-N(6)	124.97(8)
N(5)-Co(1)-N(6)	110.72(12)	N(10)-Co(2)-N(15)	111.22(11)	N(5)-Co(1)-N(6)	109.83(8)
N(7)-Co(1)-N(3)	177.25(13)	N(16)-Co(2)-N(12)	177.63(12)	N(7)-Co(1)-N(3)	176.15(9)
N(1)-Co(1)-N(3)	77.45(11)	N(14)-Co(2)-N(12)	76.37(12)	N(1)-Co(1)-N(3)	75.84(8)
N(5)-Co(1)-N(3)	77.61(11)	N(10)-Co(2)-N(12)	76.96(11)	N(5)-Co(1)-N(3)	76.53(7)
N(6)-Co(1)-N(3)	81.48(12)	N(15)-Co(2)-N(12)	81.39(11)	N(6)-Co(1)-N(3)	81.16(7)

[Co(NCO)(dbdmp)]PF_6 (4)		[Co(NCO)(dbdmp)]ClO_4 (6)		[Co(NCS)(dbdmp)]ClO_4 (9)	
N(7)-Co(1)-N(1)	105.66(16)	N(7)-Co(1)-N(1)	104.84(9)	N(7)-Co(1)-N(1)	104.66(13)
N(7)-Co(1)-N(5)	102.35(15)	N(7)-Co(1)-N(5)	102.35(10)	N(7)-Co(1)-N(5)	1024.56(14)
N(1)-Co(1)-N(5)	119.04(14)	N(1)-Co(1)-N(5)	112.73(8)	N(1)-Co(1)-N(5)	113.29(12)
N(7)-Co(1)-N(6)	98.54(16)	N(7)-Co(1)-N(6)	99.53(19)	N(7)-Co(1)-N(6)	95.92(13)
N(1)-Co(1)-N(6)	118.25(13)	N(1)-Co(1)-N(6)	109.45(7)	N(1)-Co(1)-N(6)	122.76(11)
N(5)-Co(1)-N(6)	109.37(14)	N(5)-Co(1)-N(6)	124.76(8)	N(5)-Co(1)-N(6)	111.94(12)
N(7)-Co(1)-N(3)	178.41(15)	N(7)-Co(1)-N(3)	178.13(9)	N(7)-Co(1)-N(3)	175.78(13)
N(1)-Co(1)-N(3)	75.88(12)	N(1)-Co(1)-N(3)	76.58(7)	N(1)-Co(1)-N(3)	76.97(10)
N(5)-Co(1)-N(3)	77.07(13)	N(5)-Co(1)-N(3)	73.91(7)	N(5)-Co(1)-N(3)	78.08(11)
N(6)-Co(1)-N(3)	80.31(12)	N(6)-Co(1)-N(3)	81.04(7)	N(6)-Co(1)-N(3)	79.99(10)

Molar conductivity measurement in CH_3CN solution (~10^{-3} M) shows all the complexes are 1:1 electrolyte (Λ_M ~ 120 $\Omega^{-1}cm^2\ mol^{-1}$) and there was no change of molar conductivity even after 2 h indicating no dissociation of the complexes in the solution. The presence of counter anion was confirmed by IR spectra and single crystal X-ray diffraction studies. All complexes gave satisfactory microanalysis results confirming their composition. The complexes are soluble in a range of common organic solvents like acetonitrile, methanol, ethanol, acetone etc but insoluble in water.

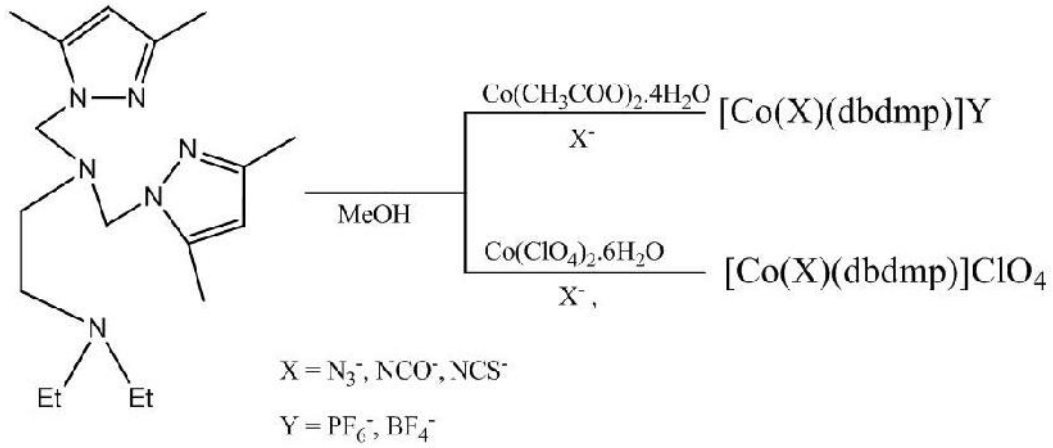

Scheme 4.1. Syntheses of complexes.

4.4.2. Description of Crystal Structures

4.4.2.1. $[Co(N_3)(dbdmp)]PF_6$ (1) and $[Co(N_3)(dbdmp)]ClO_4$ (3)

An ORTEP view with atom numbering scheme of cationic part of the mononuclear cobalt(II) complexes **1** and **3** are shown in Fig.4.1 and 4.2. Selected bond lengths and angles relevant to the coordination sphere are listed in Table 4.2. Complex **1** crystallize in monoclinic chiral space group C_2 which consists of two crystallographically independent $[Co(N_3)(dbdmp)]^+$ complex cations and two PF_6^- anions in the asymmetric unit whereas compound **3** crystallize in monoclinic space group $P2_1/c$ which consist of $[Co(N_3)(dbdmp)]^+$ and ClO_4^- ion.

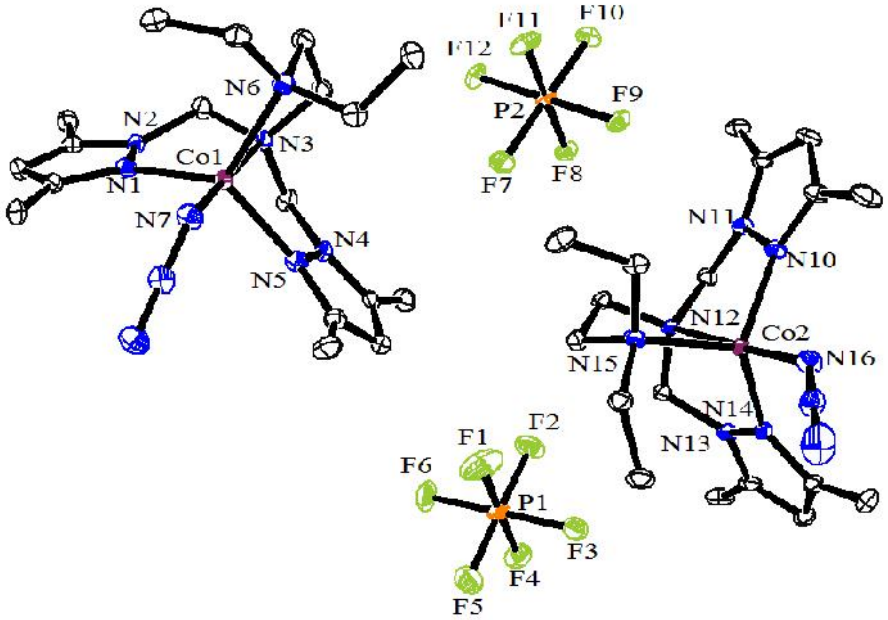

Fig.4.1. ORTEP diagram of the complex **1** with atom numbering scheme (30% probability factor for the thermal ellipsoids, H-atoms were omitted for clarity).

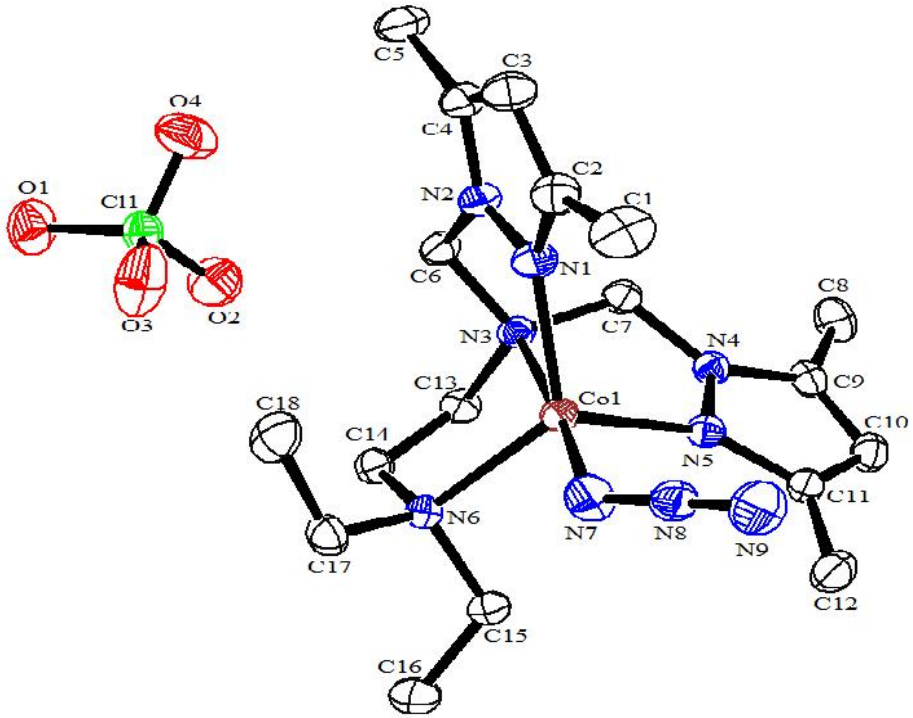

Fig.4.2. ORTEP diagram depicting the complex **3** with atom numbering scheme (30% probability factor for the thermal ellipsoids, H-atoms were omitted for clarity).

The cobalt(II) centre adopts slightly distorted trigonal bipyramidal coordination geometry with CoN_5 coordination environment in both the complexes, which is revealed by the magnitude of the trigonality index (τ = 0.96 and 0.85 for complexes **1** and **3**, respectively) [36]. Four nitrogen atoms [N(1), N(3), N(5) and N(6)] of the tetradentate ligand in combination with one nitrogen atom [N(7)] of azide ion completed trigonal bipyramidal geometry of the cobalt center. The equatorial positions are occupied by three nitrogen atoms of tetradentate ligand i.e. two nitrogen atoms [N(1), N(5)] from two pyrazole rings and one nitrogen atom [N(6)] from tertiary amine while another tertiary amine [N(3)] of ligand dbdmp and nitrogen atom from azide [N(7)] are placed at axial positions. The equatorial bond distances of Co(1)-N(1), Co(1)-N(5) and Co(1)-N(6) are in the range of 2.036(3)-2.124(4) Å and they are nearly equal but the two axial distances of Co(1)-N(3) [2.256(3) Å for **1** and 2.2435(19) Å for **2**] is longer than that of Co(1)-N(7) [2.001(3) Å for **1** and 1.999(2) Å for **2**]. The cobalt-tertiary amine bond lengths are most elongated and comparable to reported cobalt(II) complex with ligand dbdmp [2.252(4) Å] [37] and cobalt(II) chloride complex with tripodal ligand tris(2-pyridylmethyl)amine (TPA) [2.2841(18) Å] [38]. The equatorial bond angles are in the range of 109.83(8)-119.29(12)º whereas axial bond angle N(3)-Co(1)-N(7) is 177.25(13)º and 176.15(9)º for **1** and **3**, respectively.

4.4.2.2. $[Co(NCO)(dbdmp)]PF_6$ (4) and $[Co(NCO)(dbdmp)]ClO_4$ (6)

An ORTEP view with atom numbering scheme of the mononuclear cobalt(II) complexes **4** and **6** are shown in Fig.4.3 and Fig.4.4, respectively. The complex **4** crystallize in orthorhombic chiral space group $P2_12_12_1$ whereas complex **6** crystallize in monoclinic space group $P2_1/c$. For the complexes **4** and **6**, cobalt(II) center adopts a distorted trigonal bipyramidal geometry (τ = 0.99 for **4** and 0.89 for **6**) with CoN_5 coordination environment, respectively. In the complexes **4** and **6**, four nitrogen atoms N(1), N(3), N(5) and N(6) of the tetradentate ligand dbdmp in combination with one nitrogen atom [N(7)] of NCO^- ion completed trigonal bipyramidal coordination of the metal ion.

The equatorial positions are occupied by three nitrogen atoms of tetradentate ligand i.e. nitrogen atoms N(1), N(5) of the pyrazole rings and nitrogen atom N(6) of

the tertiary amine while another tertiary amine N(3) of ligand and nitrogen atom N(7) of the NCO^- are placed at axial positions. The equatorial bond distances of complex **4**, Co(1)-N(1), Co(1)-N(5) and Co(1)-N(6) are in the range of 2.040(3) to 2.108(3) Å and they are nearly equal but the axial bond distance of Co(1)-N(3) (2.330(3) Å) is longer than Co(1)-N(7) (1.950(4) Å).

In the case of complex **6**, the axial bond distance Co(1)-N(3) (2.255(4) Å) is shorter than Co(1)-N(3) (2.329(3) Å) of complex **4** whereas the bond distance of Co(1)-N(7) (1.997(5) Å) of complex **6** is nearly equal to the distance of Co(1)-N(7) (1.950(4) Å) of complex **4**. The equatorial bond angles are in the range of 109.39(14)-124.76(8)º whereas axial bond angle N(3)-Co(1)-N(7) is 178.41(15)º for complex **4** and N(3)-Co(1)-N(7) is 178.13(9)º for complex **6**.

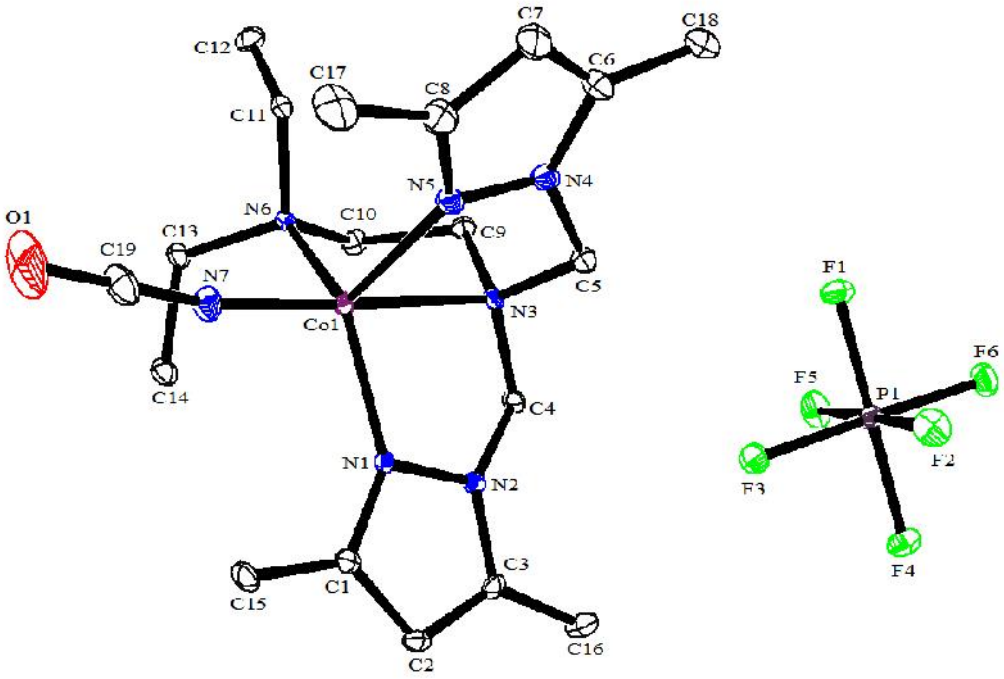

Fig.4.3. ORTEP diagram depicting the complex **4** with atom numbering scheme (30% probability factor for the thermal ellipsoids, H-atoms were omitted for clarity).

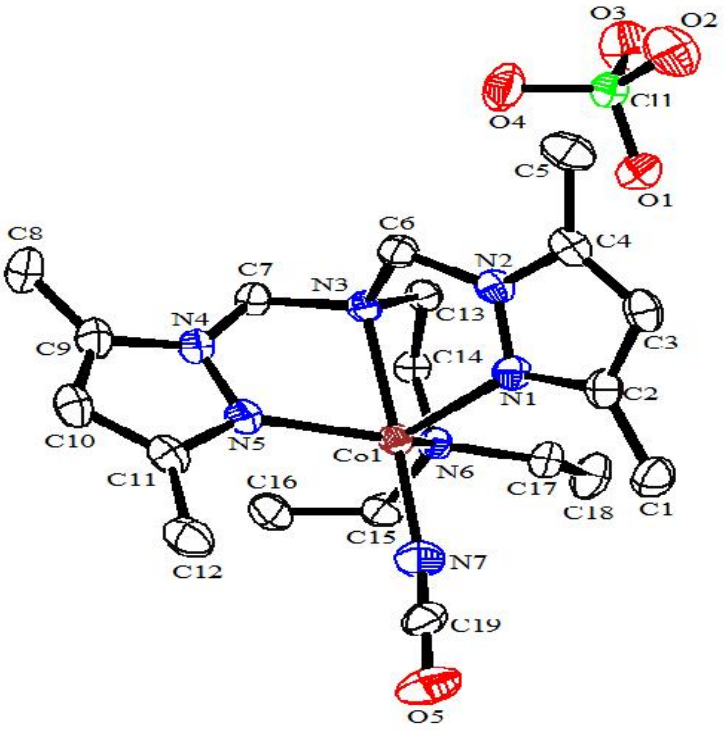

Fig.4.4. ORTEP diagram depicting the complex **6** with atom numbering scheme (30% probability factor for the thermal ellipsoids, H-atoms were omitted for clarity).

4.4.2.3. [Co(NCS)(dbdmp)]ClO_4 (9)

The complex crystallizes in monoclinic system with the space group $P2_1/c$. The ORTEP diagram of complex **9** along with the atom labeling scheme is shown in Fig.4.5. The cobalt(II) centre adopts a distorted trigonal bipyramidal coordination geometry (τ = 0.88) with CoN_5 coordination environment. Four nitrogen atoms [N(1), N(3), N(5) and N(6)] of the tetradentate ligand in combination with nitrogen atom [N(7)] of thiocyanate complete trigonal bipyramidal coordination of the cobalt(II) ion. The equatorial positions are occupied by three nitrogen atoms of tetradentate ligand i.e. pyrazole rings' nitrogen atoms [N(1), N(5)] and tertiary amine's nitrogen atom [N(6)] while another tertiary amine [N(3)] of ligand and thiocyanate's nitrogen atom [N(7)] are placed at axial positions. The equatorial bond distances Co(1)-N(1), Co(1)-N(5) and Co(1)-N(6) are in the range of 2.057(3) to 2.132(3) Å but the axial bond distance of Co(1)-N(3) [2.245(3) Å] is longer than Co(1)-N(7) [1.981(4) Å]. The equatorial bond angles are in the range of 111.94(12)-122.76(11)º whereas axial bond angle N(3)-Co(1)-N(7) is 175.78(13)º.

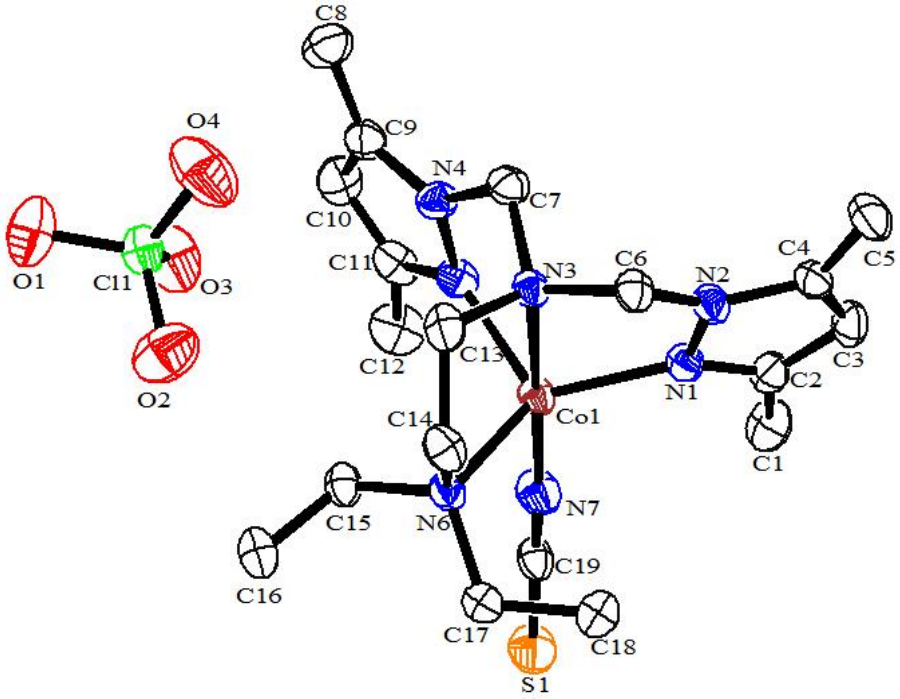

Fig.4.5. ORTEP diagram depicting the complex **9** with atom numbering scheme (30% probability factor for the thermal ellipsoids, H-atoms were omitted for clarity).

4.4.3. Spectral Data and Magnetic Studies

4.4.3.1. IR Spectra

The IR spectra of the complexes were assigned in comparison of the spectra of the ligand. All the complexes show two intense bands at ~ 1550 and ~ 1460 cm^{-1} due to ν(C = C) + ν (C = N) of pyrazole ring and these two bands are also present in the ligand indicating the coordination of ligand dbdmp in the cobalt complexes. The complexes **1-3** exhibit a very strong band in the region ~ 2071 cm^{-1} which is assigned to asymmetric stretching vibration of N- bonded terminal ν(N_3) band. A strong band at 2229 cm^{-1} appeared for complex **4** whereas a sharp band appeared at ~2217 cm^{-1} which is assigned to N-bonded NCO^- ion for the complexes **5** and **6**, respectively and further it is confirmed by single crystal x-ray crystallography [39]. A sharp peak in the range 2067 - 2069 cm^{-1} appeared for complexes **7-9** due to N-bonded ν(NCS^-). Similarly, complexes **1**, **4**, and **7** showed a strong band at ~ 845 cm^{-1} due to ν(PF_6^-) and complexes **2**, **5** and **8** exhibited a broad band in the region of ~ 1065 cm^{-1} due to ν(BF_4^-) indicating the presence of PF_6^- and BF_4^- anion, respectively. The IR spectra of

complexes **3**, **6** and **9** exhibited a broad band at ~ 1078 cm^{-1} due to ν_{assy}(Cl-O) and a weak band at ~ 623 cm^{-1} due to δ(O-Cl-O) confirming the presence of perchlorate ion outside the coordination sphere in the complexes.

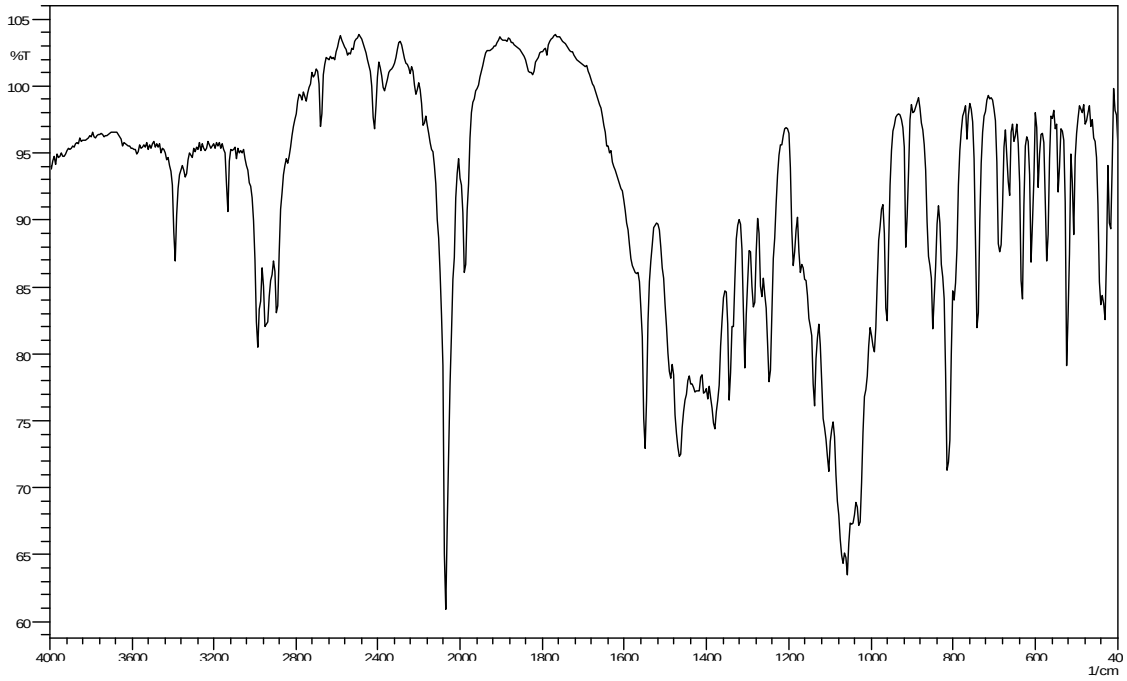

Fig.4.6. IR spectrum of $[Co(N_3)(dbdmp)]BF_4$ **(2)**.

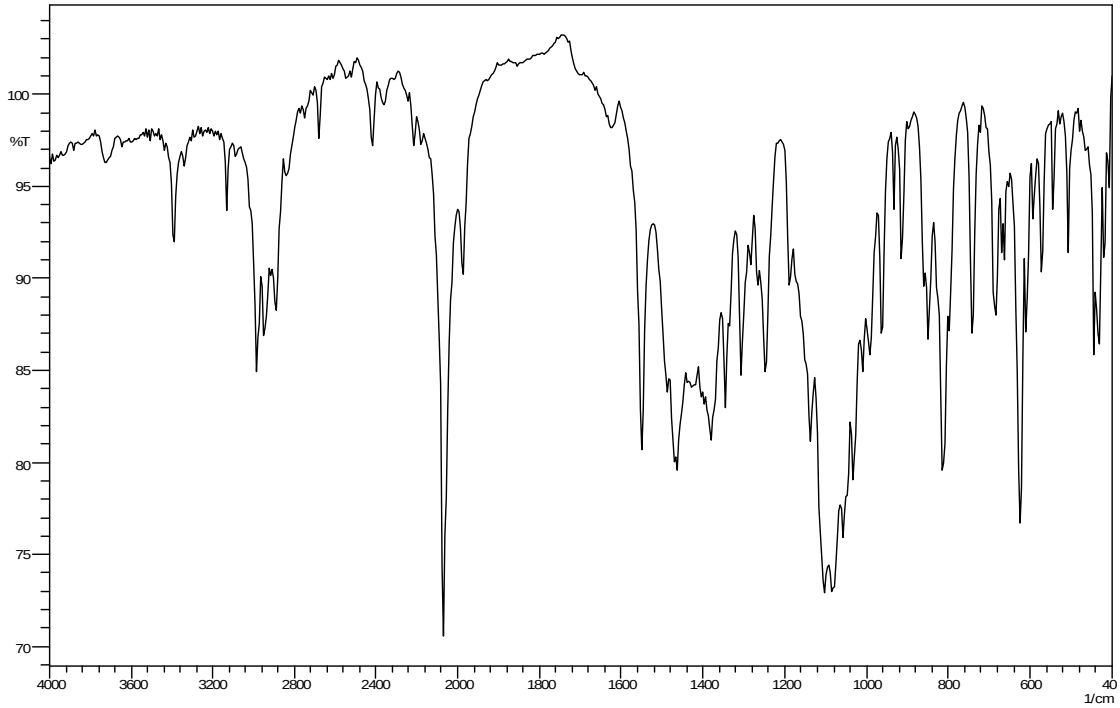

Fig.4.7. IR spectrum of $[Co(N_3)(dbdmp)]ClO_4$ **(3)**.

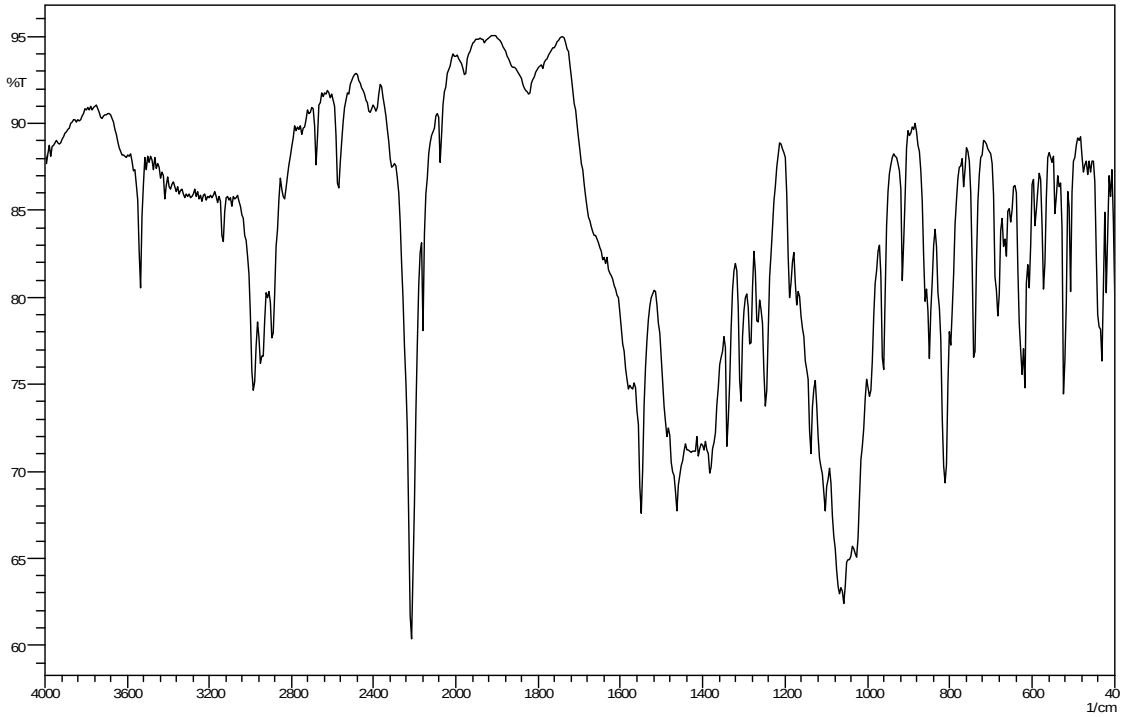

Fig.4.8. IR spectrum of $[Co(NCO)(dbdmp)]BF_4$ **(5)**.

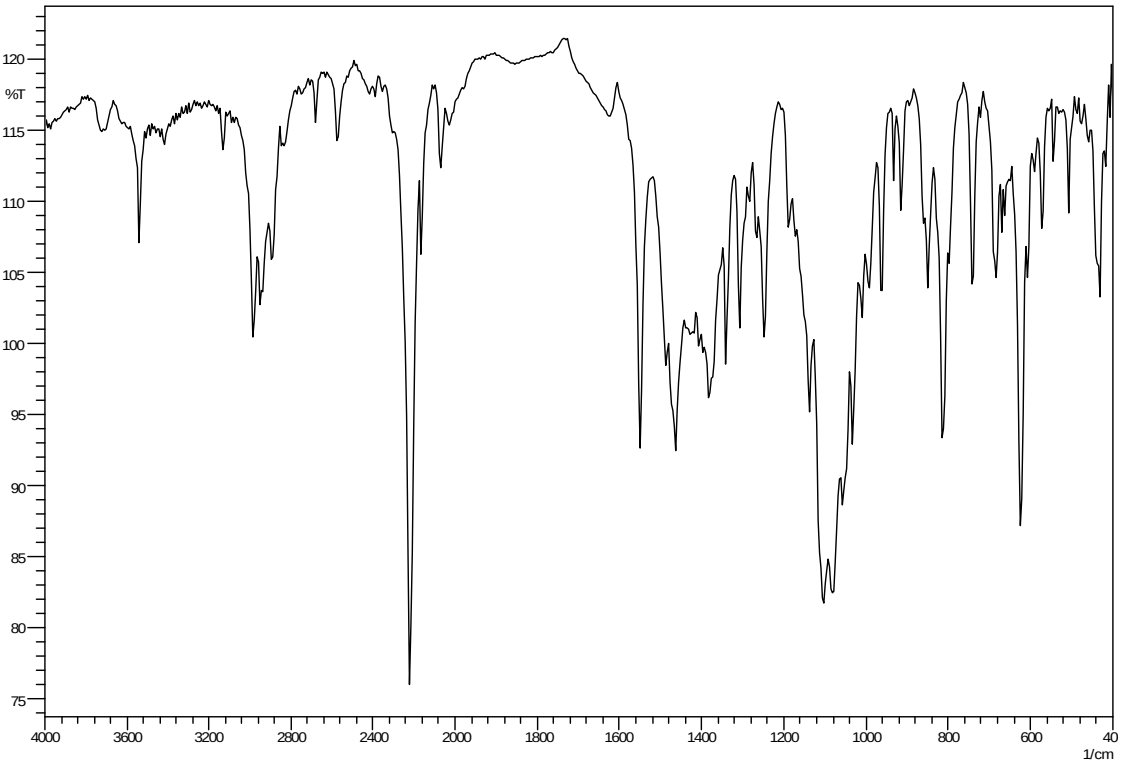

Fig.4.9. IR spectrum of $[Co(NCO)(dbdmp)]ClO_4$ **(6)**.

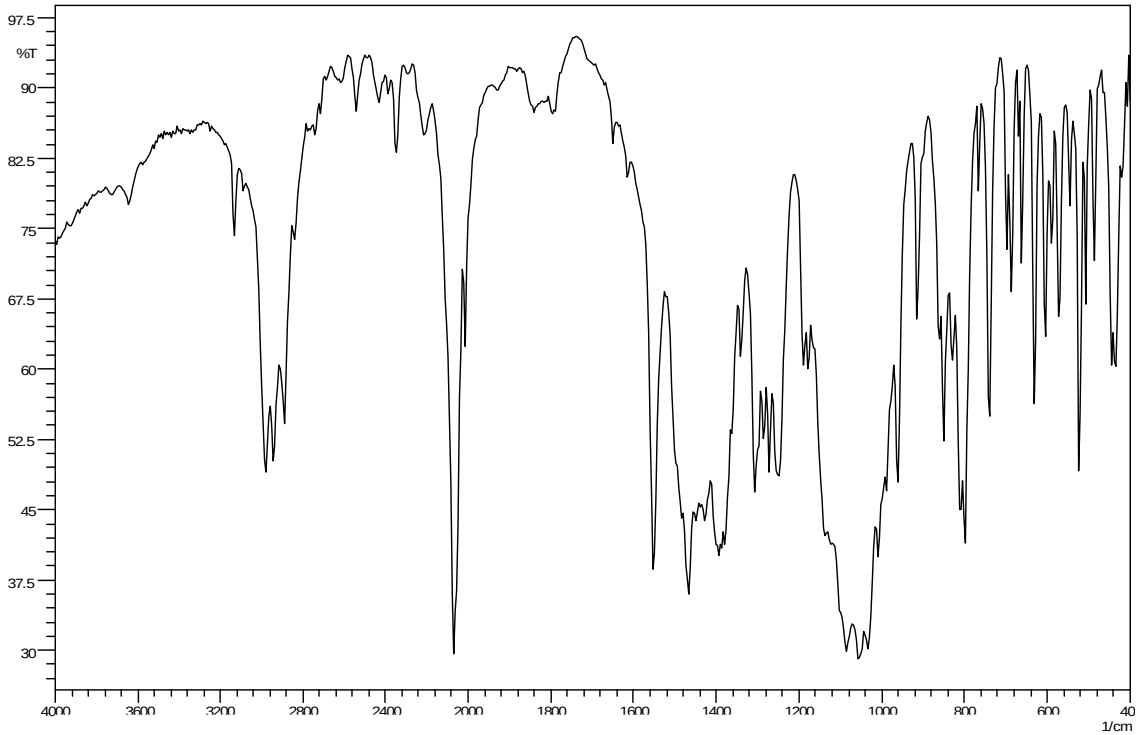

Fig.4.10. IR spectrum of $[Co(NCS)(dbdmp)]BF_4$ **(8)**.

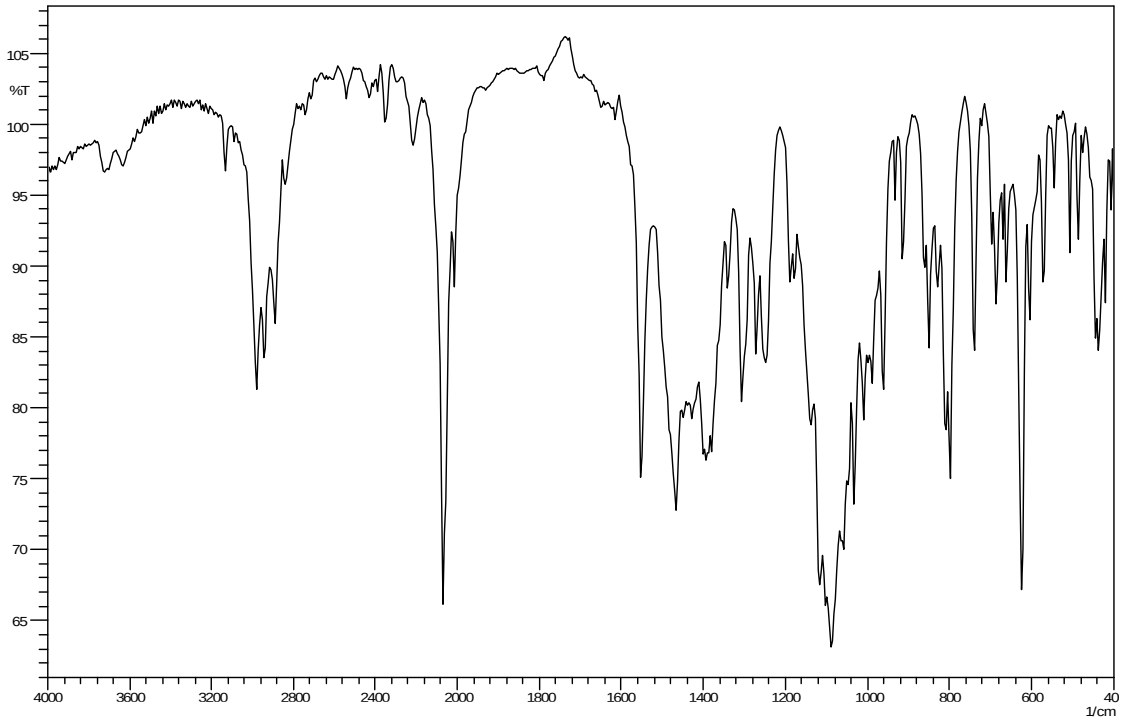

Fig.4.11. IR spectrum of $[Co(NCS)(dbdmp)]ClO_4$ **(9)**.

4.4.3.2. Electronic Spectra and magnetic data.

The complexes exhibit several absorption bands in CH_3CN in the range of 200-900 nm. The high intensity bands appeared at ~245 and ~325 nm are due to intra-ligand n-π^* / π-π^* transition. The three absorption bands appeared at ~725, ~580, ~490 nm are due to d-d transition or ligand field transitions. This type of transitions are generally observed for high spin cobalt(II) complexes with trigonal bipyramidal geometry [40].

Room temperature powder sample magnetic moment of the complexes are in the range of 4.16-32 BM indicating three unpaired electrons in the high spin cobalt(II) ion. Magnetic moment for cobalt(II) complexes with tripodal ligand fall in the range of 4.4-4.7 BM [26].

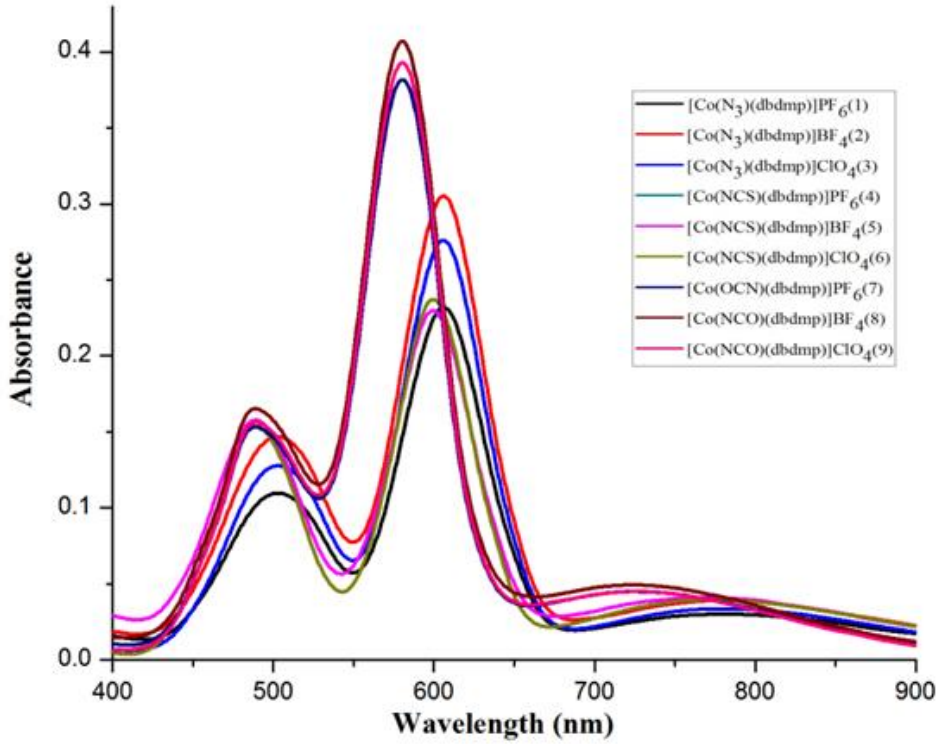

Fig.4.12. Electronic spectra of complexes **1-9** in CH_3CN at 25°C (10^{-3} M).

4.4.4. DNA and BSA Binding Study

4.4.4.1. Electronic Absorption Titration with CT-DNA

It is well-known that transition metal complexes can bind to DNA *via* both covalent and/or non-covalent interactions. In the case of covalent binding, the labile ligand of the complexes can be replaced by a nitrogen base of DNA such as guanine N7, while the non-covalent DNA interactions include intercalative, electrostatic and groove (surface) binding of metal complexes outside of DNA helix, along major or minor groove [10,41]. Hyperchromism and hypochromism are the spectral changes concerning of metal complexes association with the DNA helix. Hyperchromism means the breakage of the secondary structure of DNA, and hypochromism means the DNA-binding mode of complex is electrostatic effect or intercalation which can stabilize the DNA duplex, while the existence of a red-shift is indicative of the stabilization of DNA duplex [42]. Complex binding with DNA usually results in hypochromism and red shift arising from strong stacking interaction between complex and DNA [43-47].

The binding ability of complexes **1, 4** and **7** with CT-DNA are studied by measuring their effects using absorption spectroscopy. The absorption spectra of the cobalt(II) complexes are characterized by intense π-π* ligand based transitions in the UV and d-d transition in the visible region. The absorption spectra of complexes **1, 4** and **7** in the absence and presence of CT-DNA are presented in the Fig.4.13 and Fig.4.14, respectively. The absorption bands of d-d transitions are observed for complex **1** at 502, 607 and 781 nm. The band centered at 606 nm exhibits hypochromism by a small blue shift. Such spectral changes in d-d transitions suggest that there are some interactions like surface binding between the cobalt(II) complex and DNA [48-50]. Formation of a new band observed at 690 nm and it shows hyperchromic change which suggests that the complex could uncoil the helix structure of DNA and made more bases embedding in DNA exposed [51]. In addition, two isobestic points were observed at 642 and 722 nm which indicates the direct formation of a new complex with double-helical CT-DNA and Co(II) ion [49].

The absorption bands of d-d transitions are observed at 489, 599 and 765 nm for complex **4** and at 489, 580 and 723 nm for complex **7**. When complexes **4** and **7** are titrated with CT-DNA, hypochromism and slight blue sift is observed in UV region

whereas red shift is observed in d-d bands. In addition, three isobestic points were observed at 423, 514, and 710 nm for complex **4** and 495, 536 and 794 nm for complex **7** which indicates the direct formation of a new complex with double-helical CT-DNA [50]. The observed hypochromism and red sift suggest the stabilization of DNA duplex [42]. Such spectral changes in visible region suggest surface binding or non-covalent binding between the cobalt(II) complex and DNA [48, 50]. Recently we have reported DNA binding study of copper(II) complexes with the same ligand but no such isobestic point was observed in the UV or visible region. This also suggest new complex formation with CT-DNA and cobalt(II) complex [52].

In order to compare quantitative binding strength of studied complexes, the intrinsic binding constants K of the complexes to CT-DNA were determined by monitoring the changes of absorbance at 607 nm (for complex **1**), 485 nm (for complex **4**) and 580 nm (for complex **7**) with increasing concentration of DNA. The intrinsic binding constants K_b of complexes **1**, **4** and **7** are 2.7 (± 0.02) x 10^5, 3.93 (± 0.03) x 10^5 and 3.4 (± 0.01) x 10^5, respectively. The exact mode of binding cannot be proposed by UV spectroscopic titration studies. In most cases, the existence of hypochromism for all complexes could be considered as first evidence that the binding of the complexes involving intercalation between the base pairs of CT-DNA cannot be ruled out [53-58].

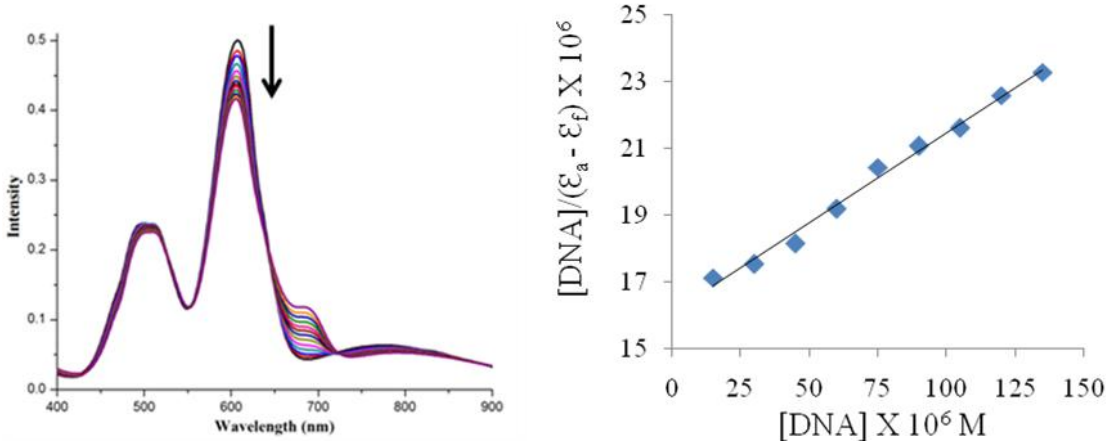

(a) **(1)**

Fig.4.13. Absorption spectra of complex **1 (a)** (1 x 10^{-3} M) in the absence and presence of increasing amount of CT-DNA (0-200 µM) at 25ºC in Tris-HCl/NaCl buffer (pH 7.2). Arrow shows the absorbance changing upon increasing DNA concentrations. Least-squares fit of [DNA]/(ε_a - ε_f) vs. [DNA] for the complexes **1 (1)**.

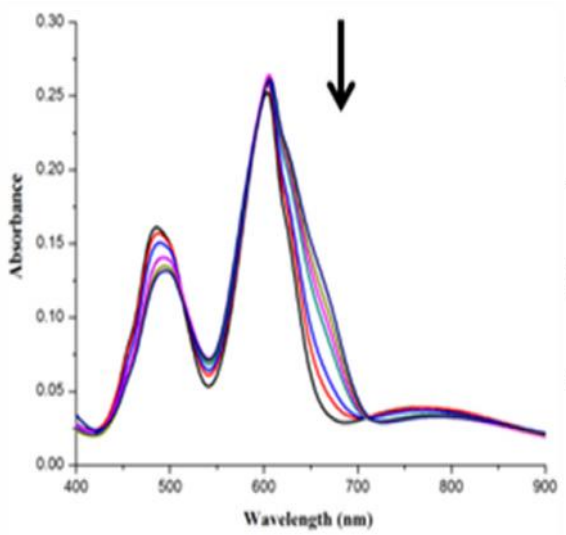

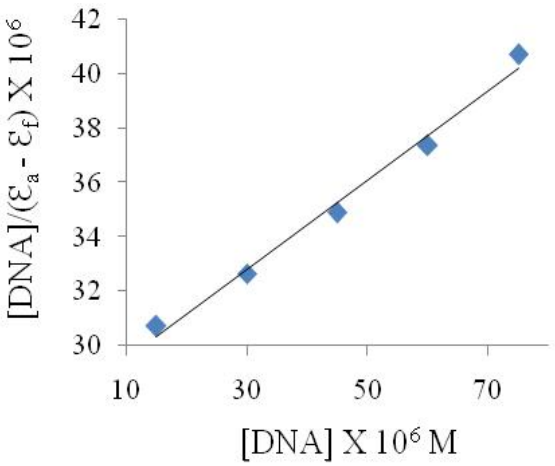

(a) **(1)**

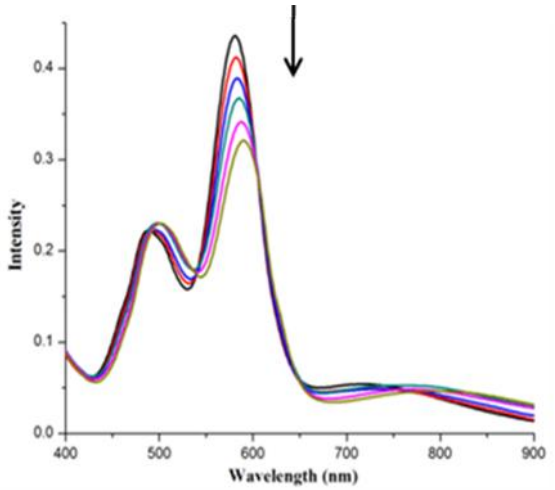

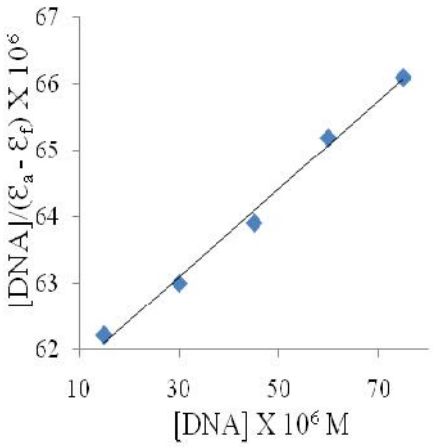

(b) **(2)**

Fig.4.14. Absorption spectra of complexes **4 (a)** and **7 (b)** (1 x 10^{-3} M) in the absence and presence of increasing amount of CT-DNA (0-200 μM) at 25°C in Tris-HCl/NaCl buffer (pH 7.2). Arrow shows the absorbance changing upon increasing DNA concentrations. Least-squares fit of [DNA]/(ε_a - ε_f) vs. [DNA] for the complexes **4(1)** and 7 **(2).**

4.4.4.2. Fluorescence spectral studies

As the present complexes are non-fluorescent at room temperature in solution or in the presence of DNA, competitive ethidium bromide binding experiments were carried out to gain support for the extent of binding with CT-DNA. The emission spectra of EB bound to DNA in the absence and presence of each complex were recorded in the Tris-buffer for [EB] = 20 μM and [DNA] = 30 μM for increasing amounts of each complex. The fluorescence quenching curves of EB-bound to DNA by the complexes **1**, **4** and **7** are shown in the Fig.4.15-4.16 and the reduction in the intensity of the emission band suggest that the complexes compete with EB and strongly bind with DNA through intercalation. The Stern–Volmer plots of DNA–EB [Fig.4.15(1)-4.15.((1), (2)] illustrate that the quenching of EB-DNA fluorescence by the compounds are in good agreement (R = 0.9) with the linear Stern–Volmer equation [53-55, 59] which also suggest the strong binding of the complexes with DNA. The Stern-Volmer quenching constant values (Table 4.3) are less than the binding constant of the classical intercalators and metallointercalators (10^7 M^{-1}) [60].

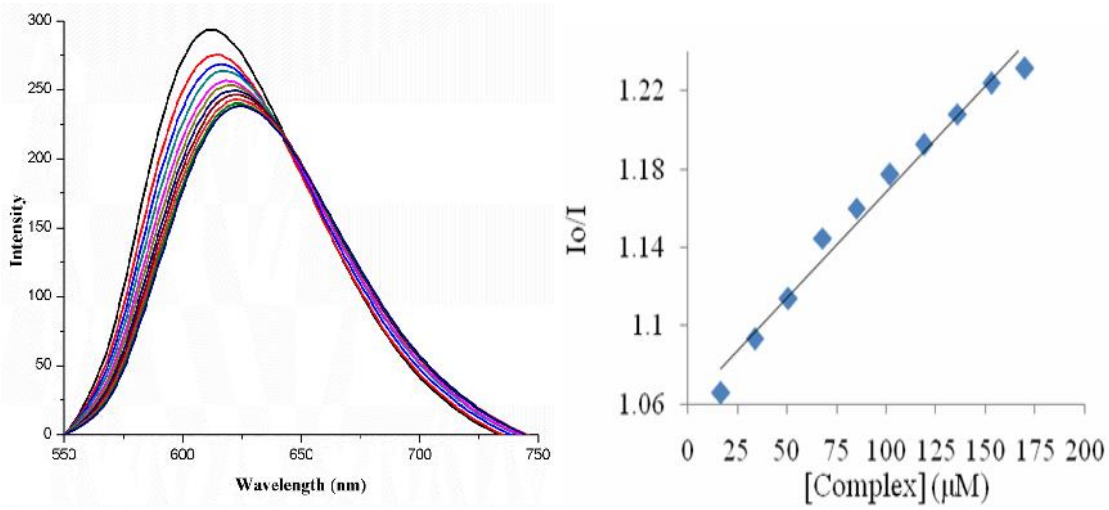

(a) (1)

Fig.4.15. Fluorescence quenching spectra of complex **1** (a) (λ_{ex} = 510 nm) by addition of increasing amount of complexes (0-160 μM) to EB-bound CT-DNA. The plot of I_o/I vs [complex] for the complex **1** (1).

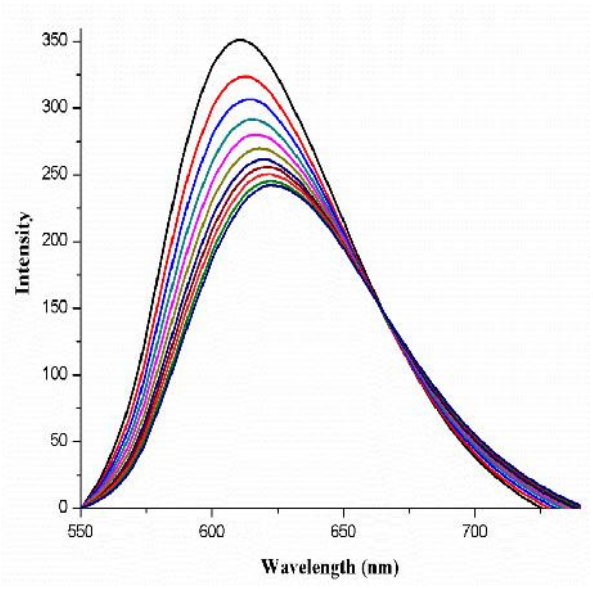

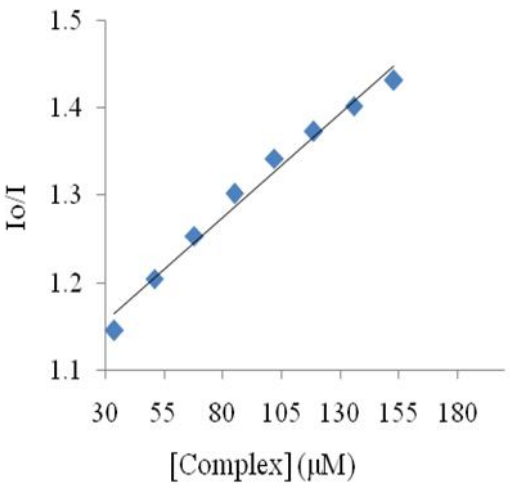

(a) (1)

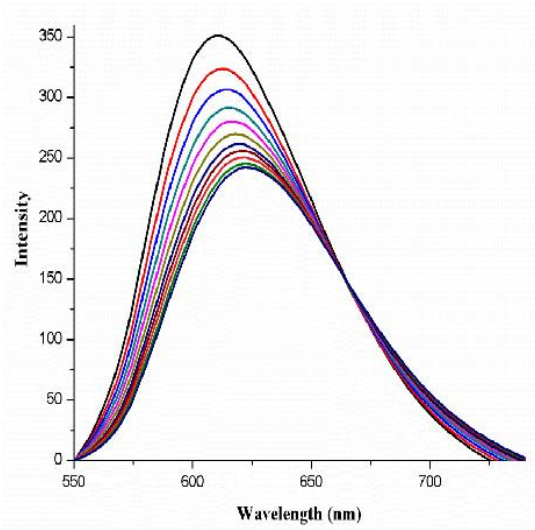

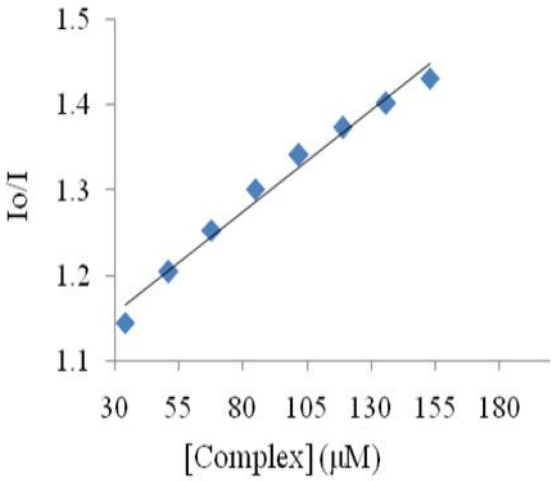

(b) (2)

Fig.4.16. Fluorescence quenching spectra of complexes **4** (a) and **7** (b) (λ_{ex} = 510 nm) by addition of increasing amount of complexes (0-160 μM) to EB-bound CT-DNA. The plot of I_o/I vs [complex] for the complexes **4** (1) and **7** (2).

4.4.4.3. Viscosity measurements

The hydrodynamic methods (i.e., viscosity and sedimentation) that are sensitive to the changes in the effective length of DNA molecules are one of the crucial tools to find the nature of binding of metal complexes to the DNA. This study was regarded as the least ambiguous and the most critical tests of binding mode in solution state in absence of crystallographic structural data [61–63]. Under the appropriate conditions intercalation results in lengthening the DNA helix as base pairs separated to accommodate the binding ligand, leading to the increase of DNA viscosity. In the case of a partial or non-classical intercalation of ligand could bend (or kink) the DNA helix and reduce its effective length, concomitantly and its viscosity [64-65].

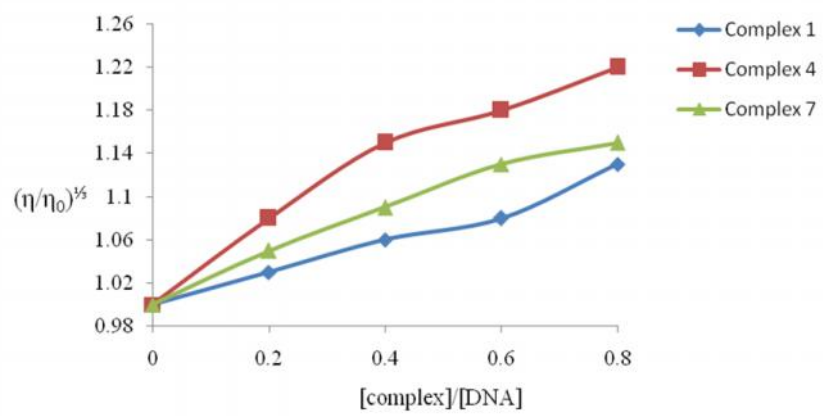

Fig.4.17. Effects of increasing amounts of complexes **1**, **4** and **7** on the relative viscosities of CT-DNA at 30±0.01°C, [DNA] = 0.5 mM.

The changes in the relative viscosity of rod-like CT-DNA in the presence of increasing amount of complexes **1**, **4** and **7** are shown in the Fig.4.17. The viscosity of DNA increases steadily with increasing concentration of the complexes. The experimental results suggest that complexes bind to DNA through a classical intercalation mode. However, this increase is relatively less as compared to classical intercalators EB. So, we can conclude that cobalt (II) complexes **1**, **4** and **7** strongly interact via surface binding or non-covalent binding which is supported by UV spectroscopic titration studies.

4.4.4.4. Fluorescence quenching of BSA by complexes.

Serum albumin is the most abundant protein in plasma which is involved in the transport of metal ions and metal complexes with drugs through the blood stream. Binding to these proteins may lead to loss or enhancement of biological properties of the original drug or provide paths for drug transportation [10]. Bovine serum albumin (BSA) is the most extensively studied serum albumin because of its structural homology with human serum albumin (HSA). Binding of transition metal complexes to bovine serum albumin (BSA) have also been interesting research field in chemistry, life sciences and clinical medicine as it greatly influences absorption, drug transport, storage, metabolism and excretion properties of typical drugs in vertebrates [66].

BSA solution exhibits an intense fluorescence emission band with a peak at 343 nm due to the tryptophan residue when excited at 290 nm [67]. The fluorescence emission spectra of BSA in the presence of complexes **1**, **4** and **7** were studied with increasing the concentration of the complexes and shown in Fig.4.18-4.19. The changes and quenching of fluorescence emission spectra upon addition of complexes **1**, **4** and **7** may be due to changes in protein conformation, subunit association, substrate binding or denaturation because of the complex binding [68].

The fluorescence quenching is described by the Stern-Volmer equation: $I_o/I = 1 + K_{sv}[Q]$, where I_o and I are the emission intensities in the absence and presence of the complexes, respectively and K_{sv} is the dynamic quenching constant and [Q] is the total concentration of complexes. The calculated values of K_{sv} for complexes **1**, **4** and **7** are 2.8 (± 0.01) x 10^3, 3.0 (± 0.09) x 10^3 and 2.7 (± 0.06) x 10^3 M^{-1}, respectively which are obtained by the slope of the Stern-Volmer plot indicating the good binding propensity. These binding constant values are lower than that of the avidin-ligands binding affinity ($K_{avidin\text{-}ligands} \cong 10^{15}$ M^{-1}) which is among highest observed so far [69]. In comparison of studied complexes (Table 4.3), complex **4** show higher binding affinity for BSA than complexes **1** and **7**. So the interaction of complexes **1**, **4** and **7** with bovine serum albumin may provide useful information for any potential application.

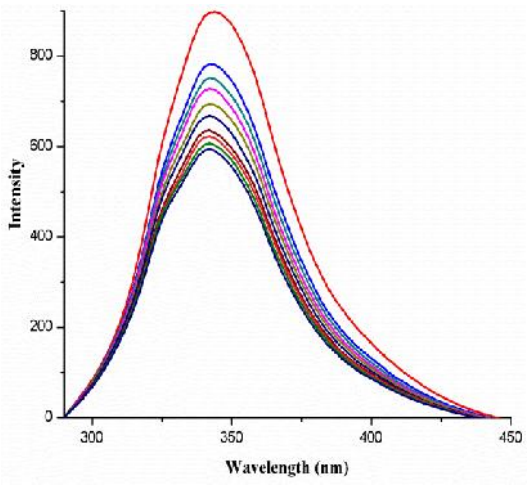

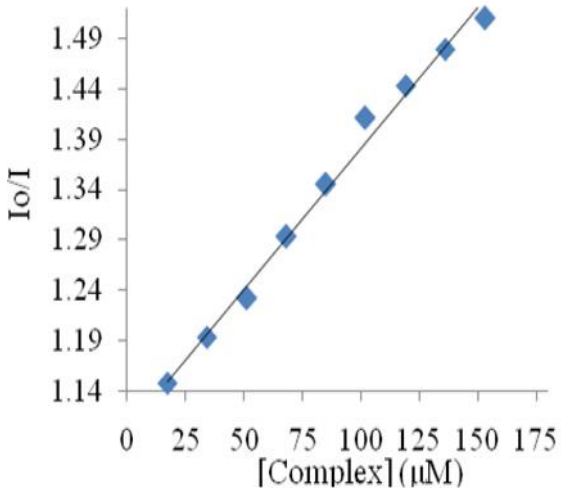

(a) **(1)**

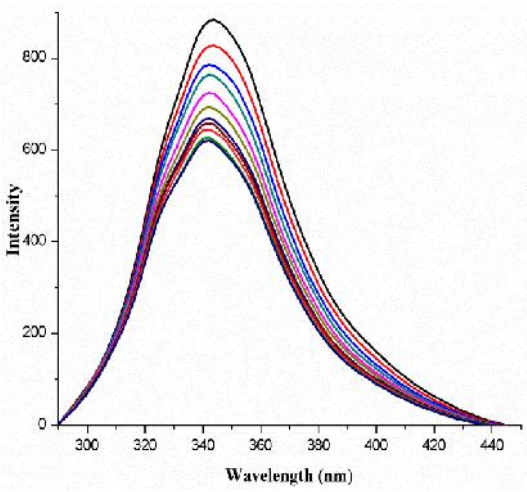

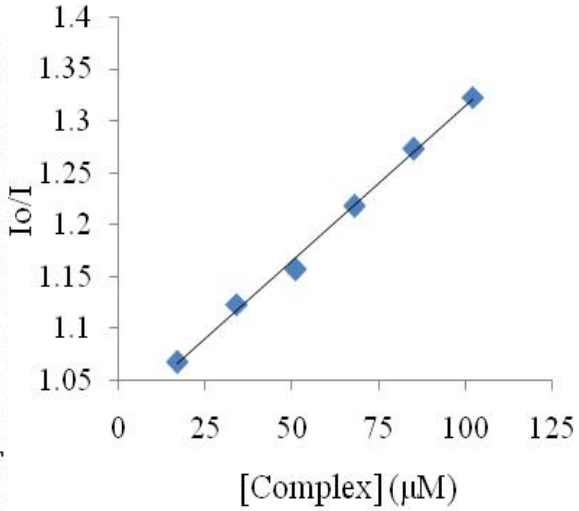

(b) **(2)**

Fig.4.18. Fluorescence quenching spectra of BSA (3 ml, 50 μM) for complexes **1** (a) and **4** (b) with increasing amount of complexes (0-300 μM) in Tris-HCl/NaCl buffer (pH 7.2) at 25ºC. Stern – Volmer plot for the quenching of BSA fluorescence by complexes **1** (1) and **4** (2).

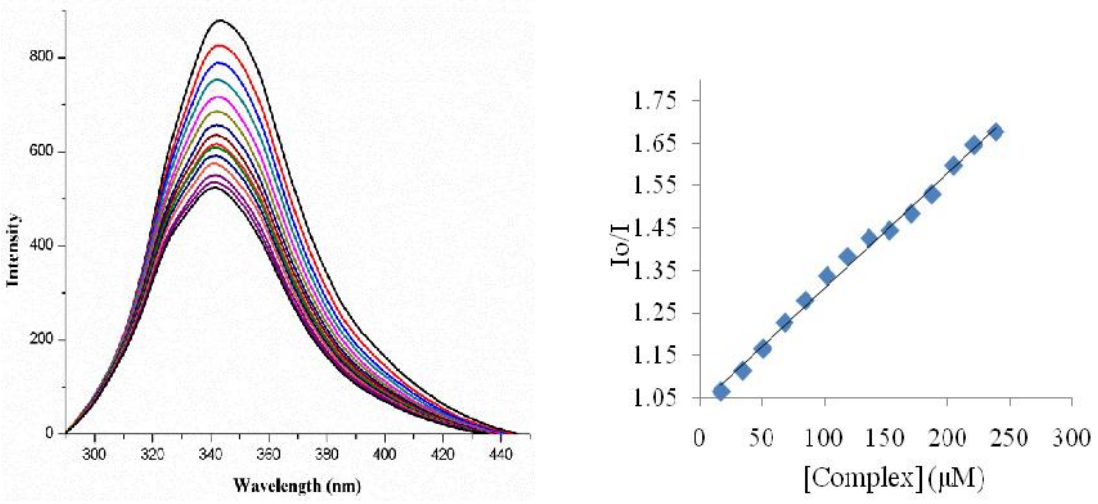

(a) **(1)**

Fig.4.19. Fluorescence quenching spectra of BSA (3 ml, 50 μM) for complex **7** (a) with increasing amount of complex (0-300 μM) in Tris-HCl/NaCl buffer (pH 7.2) at 25ºC. Stern – Volmer plot for the quenching of BSA fluorescence by complex **7** (1).

Table.4.3. Binding parameters of complexes.

Complex	K_b (M^{-1})	K_{sv} (M^{-1})	K_{sv} (BSA) (M^{-1})
(1)	2.7 (± 0.02) x 10^5	1.1 (± 0.06) x 10^3	2.8 (± 0.01) x 10^3
(4)	3.93 (± 0.03) x 10^5	2.4 (± 0.01) x 10^3	3.0 (± 0.09) x 10^3
(7)	3.4 (± 0.01) x 10^5	1.3 (± 0.07) x 10^3	2.7 (± 0.06) x 10^3

4.5. Conclusions

Mononuclear five coordinated cobalt(II) complexes of the type [Co(X)(dbdmp)]Y, where dbdmp = *N*,*N*-diethyl-*N'*,*N'*-bis((3,5-dimethyl-*1H*-pyrazol-1-yl)methyl)ethane-1,2-diamine, X = N_3^- / NCO^- / NCS^- and Y = ClO_4^- / PF_6^- / BF_4^- have been synthesized and characterized. Structural studies show all the complexes have distorted trigonal bipyramidal geometry and N_3^- and NCO^- containing cobalt(II) complexes with PF_6^- counter ion have chiral space group whereas complexes with ClO_4^- ions have non chiral space group. CT-DNA binding study of the cobalt(II) complexes were investigated by absorption, fluorescence spectroscopy and viscosity measurements and BSA binding study by fluorescence spectroscopy. The results indicate that the complexes can interact strongly with DNA base pair and protein.

4.6. References:

1. A. M. Pyle, E. C. Long, J. K. Barton, *J. Am. Chem. Soc.* 111 (1989) 4520.
2. A. Sitlani, E. C. Long, A. M. Pyle, J. K. Barton, *J. Am. Chem. Soc.* 114 (1992) 2303.
3. L. Jin, P. Yang, *Polyhedron* 16 (1997) 3395.
4. Y.-M. Song, X.-I. Liu, M.-I. Yang, X.-R. Zheng, *Transition Met. Chem.* 30 (2005) 499.
5. X. L. Wang, H. Chao, H. Li, X. L. Hong, Y. J. Liu, L. F. Tan, L. N. Ji, *J. Inorg. Biochem.* 98 (2004) 1143.
6. S. Ramakrishnan, E. Suresh, A. Riyasdeen, M. A. Akbarsha, M. Palaniandavar, *Dalton Trans.* 40 (2011) 3524.
7. S. Budagumpi, N. V. Kulkarni, G. S. Kurdekar, M. P. Sathisha, V. K. Revankar, *Eur. J. Med. Chem.* 45 (2010) 455.
8. M. N. Patel, M. R. Chhasatia, D. S. Gandhi, *Bioorg. Med. Chem. Lett.* 19 (2009) 2870.
9. E. K. Efthimiadou, A. Karaliota, G. Psomas, *Bioorg. Med. Chem. Lett.* 18 (2008) 4033.
10. F. Dimiza, A. N. Papadopoulos, V. Tangoulis, V. Psycharis, C. P. Raptopoulou, D. P. Kessissoglou, G. Psomas, *Dalton Trans.* 39 (2010) 4517.
11. F. Zhang, Q. Y. Lin, W. D. Liu, P. P. Wang, W. J.Song, B-W. Zheng, *J. Coord. Chem.* 66 (2013) 2297.
12. X. Fan, J. Dong, R. Min, Y. Chen, X. Yi, J. Zhou, S. Zhang, *J. Coord. Chem.* 66 (2013) 4268.
13. B. Li, W. Liu, J. Shao, C. L. Xue, C. Z. Xie, Y. Ouyang, J. Y. Xu, *J. Coord. Chem.* 66 (2013) 2465.
14. T.-F. Miao, S. Li, Jun Li, K.-C. Zheng, *J. Inorg. Biochem.* 109 (2012) 16.
15. B. Peng, H. Chao, B. Sun, H. Li, F. Gao, L.-N. Ji, *J. Inorg. Biochem.* 101 (2007) 404.
16. A. Panja, *Polyhedron* 43 (2012) 22.
17. R. S. Kumar, S. Arunachalam, *Polyhedron* 25 (2006) 3117.
18. M. F. Reichmann, S. A. Rice, C. A. Thomas, P. Doty, *J. Am. Chem. Soc.* 76 (1954) 3047.

19. O. Gia, S. M. Magno, H. Gonzalaz-Diaz, E. Quezada, L. Santana, E. Uriarte, L. Dalla Via, *Bioorg. Med. Chem.* 13 (2005) 809.
20. J. R. Lakowicz, *Principles of Fluorescence Spectroscopy, 2nd ed. Plenum Press, New York* (1999).
21. G. M. Sheldrick, *SAINT, 5.1 ed. Siemens Industrial Automation Inc., Madison, WI* (1995).
22. Agilent (2011). *CrysAlis PRO*. Agilent Technologies UK Ltd, Yarnton, England.
23. G. M. Sheldrick. *SADABS, Empirical Absorption Correction Program, University of Gottingen, Gottingen, Germany* (1997).
24. G. M. Sheldrick, *SHELXTL Reference Manual (Version 5.1), Bruker AXS, Madison, WI* (1997).
25. G. M. Sheldrick. SHELXL-97: *Program for Crystal Structure Refinement, University of Gottingen, Gottingen* (1997).
26. S. Sabiah, B. Varghese, N. N. Murthy, *Dalton Trans.* (2009) 9770.
27. J. R. Cubanski, S. A. Cameron, J. D. Crowley, A. G. Blackman, *Dalton Trans.* 42 (2013) 2174.
28. S. S. Massoud, F. R. Louka, Y. K. Obaid, R. Vicente, J. Ribas, R. C. Fischerc, F. A. Mautner, *Dalton Trans.* 42 (2013) 3968.
29. F. A. Saad, N. J. Buurma, A. J. Amoroso, J. C. Knight, B. M. Kariuki, *Dalton Trans.* 41 (2012) 4608.
30. S. S. Massoud, L. L. Quan, K. Gatterer, J. H. Albering, R. C. Fischer, F. A. Mautner, *Polyhedron* 31 (2012) 601.
31. S. S. Massoud, K. T. Broussard, F. A. Mautner, R. Vicente, M. K. Saha, I. Bernal, *Inorg. Chim. Acta* 361 (2008) 123.
32. S. B. Kumar, M. Zala, A. Solanki, M. Rangrez, P. Parikh, E. Suresh, *Polyhedron* 36 (2012) 15.
33. C. J. Davies, G. A. Solan, J. Fawcett, *Polyhedron* 23 (2004) 3105.
34. A. Garoufis, S. Kasselouri, C.P. Raptopoulou, *Inorg. Chem. Commun.* 3 (2003) 251.
35. T. M. Kooistra, K. F. W. Hekking, Q. Knijnenburg, B. de Bruin, P. H. M. Budzelaar, R. Gelder, J. M. M. Smits, A. W. Gal, *Eur. J. Inorg. Chem.* 4 (2003) 648.

36. A. W. Addision, T. N. Rao, J. Reedijk, J. Van Rijn, G. C. Verschoor, *J. Chem. Soc., Dalton Trans.* (1984) 1349.
37. A. Solanki, S. B. Kumar, *Polyhedron* 81 (2014) 323.
38. C. J. Davies, G. A. Solan, J. Fawcett, *Polyhedron* 23 (2004) 3105.
39. K. Nakamoto, *Infrared and Raman Spectra of Inorganic and Coordination compounds, Willey-Interscience, New York*, (1986).
40. G. Achilleas, K. Spyridoula and P. R. Catherine, *Inorg. Chem.Commun.* 3 (2000) 251.
41. Q. Zhang, J. Liu, H. Chao, G. Xue, L. Ji, *J. Inorg. Biochem.* 83 (2001) 49.
42. E. C. Long, J. K. Barton, *Acc. Chem. Res.* 23 (1990) 271.
43. C. Hiort, P. Lincoln, B. Norden, *J. Am. Chem. Soc.* 115 (1993) 3448.
44. L. Fin, P. Yang, *J. Inorg. Biochem.* 68 (1997) 79.
45. Mudasir, K. Wijaya, D. H. Tjahjono, N. Yoshioka, H. Inoue, *Z. Naturforsch.* 59b (2004) 310.
46. M. Navarro, E. J. Cisneros-Fajardo, M. Fernandez-Mestre, D. Arrieche, E. Marchan, *J. Biol. Inorg. Chem.* 8 (2003) 401.
47. R. B. Nair, E. S. Teng, S. L. Kirkland, C. J. Murphy, *Inorg. Chem.* 37 (1998) 139.
48. P. T. Selvi, H. S. - Evans, M. Palaniandavar, *J. Inorg. Biochem.* 99 (2005) 2110.
49. A. Ray, B. K. Seth, U. Pal, S. Basu, *Spectrochim. Acta Part A* 92 (2012) 164.
50. K. Ghosh, P. Kumar, N. Tyagi, *Inorg. Chim. Acta* 357 (2011) 77.
51. G. Pratviel, J. Bernadou, B. Meunier, *Adv. Inorg. Chem.* 45 (1998) 251.
52. A. Solanki, S. B. Kumar, A. A. Doshi, C. Ratna Prabha, *Polyhedron* 63 (2013) 147.
53. K. C. Skyrianou, F. Perdih, I. Turel, D. P. Kessissoglou, G. Psomas, *J. Inorg. Biochem.* 104 (2010) 161.
54. K. C. Skyrianou, V. Psycharis, C. P. Raptopoulou, D. P. Kessissoglou, G. Psomas, *J. Inorg. Biochem.* 105 (2011) 63.
55. A. Tarushi, C. P. Raptopoulou, V. Psycharis, A. Terzis, G. Psomas, D. P. Kessissoglou, *Bioorg. Med. Chem.* 18 (2010) 2678.
56. G. Psomas, A. Tarushi, E. K. Efthimiadou, Y. Sanakis, C. P. Raptopoulou, N. Katsaros, *J. Inorg. Biochem.* 100 (2006) 1764.

57. A. Tarushi, G. Psomas, C. P. Raptopoulou, D. P. Kessissoglou, *J. Inorg. Biochem.* 103 (2009) 898.
58. B. C. Baguley, M. Lebret, *Biochemistry* 23 (1984) 937.
59. G. Psomas, *J. Inorg. Biochem.* 102 (2008) 1798.
60. M. Cory, D. D. McKee, J. Kagan, D. W. Henry, J. A. Miller, *J. Am. Chem. Soc.* 107 (1985) 2528.
61. S. Zhang, Y. Zhu, C. Tu, H. Wei, Z. Yang, L. Lin, J. Ding, J. Zhang, Z. Guo, *J. Inorg. Biochem.* 98 (2004) 2099.
62. V. A. Izumrudov, M. V. Zhiryakova, A. A. Goulko, *Langmuir*, 18 (2002) 10348.
63. J. Liu, T. Zhang, T. Lu, L. Qu, H. Zhou, Q. Zhang, L. Ji, *J. Inorg. Biochem.* 91 (2002) 269.
64. S. Satyanarayana, J. C. Dabroniak, J. B. Chaires, *Biochemistry* 31 (1992) 9319.
65. S. Satyanarayana, J. C. Dabroniak, J. B. Chaires, *Biochemistry* 32 (1993) 2573.
66. Y. Z. Zhang, H. R. Li, J. Dai, W. J. Chen, J. Zhang, Y. Liu, *Biol. Trace Elem. Res.* 135 (2010) 136.
67. J. R. Lakowicz, *Principles of Fluorescence Spectroscopy, 2nd ed. Plenum Press, New York* (1999).
68. Y. Wang, H. Zhang, G. Zhang, W. Tao, S. Tang, *J. Luminesc.* 126 (2007) 211.
69. E. Chalkidou, F. Perdih, I. Turel, D. P. Kessissoglou, G. Psomas, *J. Inorg. Biochem.* 113 (2012) 55.